AD NUMBER

AD855516

NEW LIMITATION CHANGE

TO

Approved for public release, distribution unlimited

FROM

Distribution authorized to U.S. Gov't. agencies and their contractors; Administrative/Operational use; Jun 1969. Other requests shall be referred to Air Force Weapons Laboratory, Air Force Systems Command, Kirtland Air Force Base, New Mexico.

AUTHORITY

AFWL ltr, 30 Nov 1971

AFWL-TR-
68-73

CONCEPTUAL DESIGN STUDIES OF TWO TURPS USING STIRLING AND DIRECT ENERGY CONVERSION CYCLES

R. Magladry
G. F. Zindler

Isotopes
Nuclear Systems Division
Middle River, Maryland

Contract F29601-68-C-0042

TECHNICAL REPORT NO. AFWL-TR-68-73

June 1969

AIR FORCE WEAPONS LABORATORY
Air Force Systems Command
Kirtland Air Force Base
New Mexico

92

AIR FORCE WEAPONS LABORATORY
Air Force Systems Command
Kirtland Air Force Base
New Mexico

AFWL-TR-68-73

CONCEPTUAL DESIGN STUDIES OF TWO TURPS USING STIRLING AND DIRECT ENERGY CONVERSION CYCLES

R. Magladry

G. F. Zindler

Isotopes
Nuclear Systems Division
Middle River, Maryland
Contract F29601-68-C-0042

TECHNICAL REPORT NO. AFWL-TR-68-73

FOREWORD

This report was prepared by Isotopes, Nuclear Systems, Division, Middle River, Maryland under Contract F29601-68-C-0042. The research was performed under Program Element 6.24.05.21.F, Project 3145, Task 24.001.

Inclusive dates of research were June 1968 through March 1969. The report was submitted 30 April 1969 by the Air Force Weapons Laboratory Project Officer, Captain Bertrand F. Ruggles (WLDC).

Information in this report is embargoed under the U.S. Export Control Act of 1949, administered by the Department of Commerce. This report may be released by departments or agencies of the U.S. Government to departments or agencies of foreign governments with which the United States has defense treaty commitments, subject to approval of AFWL (WLDC).

This report has been reviewed and is approved.

Bertrand F. Ruggles
BERTRAND F. RUGGLES
Captain, USAF
Project Officer

CLIFF M. WHITEHEAD
Colonel, USAF
Chief, Civil Engineering Branch

GEORGE C. DARBY, JR.
Colonel, USAF
Chief, Development Division

ABSTRACT

(Distribution Limitation Statement No. 2)

This report presents designs of two compact, unattended nuclear power plants utilizing H-Rho reactor control. One plant is a 100-kilowatt(e) system with Stirling cycle conversion; the other is a conduction-cooled 10-kilowatt(e) thermoelectric system. The conduction system is based upon current technology, while the Stirling system requires an extended life Stirling engine for optimal performance.

In addition to the performance the results of parametric studies of system operation at other power levels are included.

This report shows that reliable, unattended power can be obtained at moderate cost. The Stirling conversion plant achieves high efficiency and compactness by using the reactor coolant as the engine working fluid. The direct conduction plant provides very long operating life by eliminating moving parts and coolant.

CONTENTS

Section		Page
I	INTRODUCTION	1
II	H-RHO REACTOR-STIRLING ENGINE POWER PLANT	3
III	DIRECT CONDUCTION REACTOR-THERMOELECTRIC POWER PLANT	37
IV	REFERENCES	75
Appendix		
	HYDROGEN REACTIVITY CONTROL (H-RHO)	77
	Distribution	85

ILLUSTRATIONS

Figure		Page
1	Installation of H-Rho-Stirling Power System	8
2	H-Rho Reactor Compartment for Stirling Engine System	9
3	Core Diameter and Fuel Loading Variations with Fuel Matrix Weight Percent Uranium for 5-Year Operation at 400 Kilowatts(t)	12
4	Relationship Between Fuel Region Thickness and Outer Diameter for 10-Year Operation at 200 Kilowatts(t)	14
5	Effect of Core Coolant Pressure Drop on Fuel Temperature for Core Power Level of 500 Kilowatts(t)	17
6	Effect of Core Coolant Volume on Average Fuel Temperature	18
7	Effect of Number of Coolant Tubes on Average Fuel Temperature	20
8	Effect of Number of Coolant Tubes on Maximum Fuel Temperature	21
9	Response to Step Change in Electrical Load from 100 to 70 Kilowatts for Stirling Engine System	25
10	Response to Step Change in Electrical Load from 70 to 100 Kilowatts for Stirling Engine System	26
11	Effect of Reprocessing Availability Rate on Fuel Cycle Cost	34
12	Installation of Direct-Conduction Reactor System	41
13	Direct-Conduction H-Rho Reactor Thermoelectric Generator	42
14	Relationship Between Fuel Region Thickness and Outer Diameter for 10-Year Operation at 200 Kilowatts(t)	45
15	Variation of Fuel Loading with Fuel Region Outer Diameter	46
16	Effect of Core Size and Fuel Composition on Thermal Capability	51

ILLUSTRATIONS (cont'd)

Figure		Page
17	Temperature Distribution Through Mid-Plane at 244 Kilowatts(t)	53
18	Temperature Distribution in Copper Conductor	54
19	Thermal Power Response of Thermoelectric System for Step Load Changes from 70 to 100% and 100 to 70% Power	56
20	Schematic of Condition-Cooled Reactor	58
21	Jacketed Thermoelectric Element for Generator of Nuclear Power System	61
22	Performance of P Element Clamped by 400 psi	63
23	Performance of Jacketed N Element	64
24	Power Conditioner	66
25	Effect of Reprocessing Rate on Fuel Cycle Cost	73
26	H-Rho Operational Principle with Hydrogen Reservoir	78

TABLES

Table		Page
I	Stirling Cycle TURPS Conceptual Design Characteristics	5
II	Fixed Parameters for Nuclear Analysis	11
III	Reactivity Inventory and Control Margin for a Five-Weight Percent Core	13
IV	Reactor-Stirling System Weight	31
V	H-Rho Reactor-Stirling Plant Cost	32
VI	Fuel Cycle Parameters, Set by Design	33
VII	Fuel Cycle Parameters, Typical Values Set by Industry	35
VIII	Fuel Cycle Parameters, Typical Values Set by AEC	35
IX	Fuel Cycle Parameters, Assumed Industrial Charges	35
X	Fuel Cycle Parameters, Assumed AEC Charges	36
XI	Fuel Cycle Cost	36
XII	Conduction-Cooled Reactor Conceptual Design Characteristics	39
XIII	Reactivity Inventory for Conduction-Cooled Core	47
XIV	Weight Estimate of Generator Components	68
XV	Production Plant Cost Estimates	69
XVI	Fuel Cycle Parameters, Set by Design	69
XVII	Fuel Cycle Parameters, Typical Values Set by Industry	70
XVIII	Fuel Cycle Parameters, Typical Values Set by AEC	70
XIX	Fuel Cycle Parameters, Assumed Industrial Charges	70
XX	Fuel Cycle Parameters, Assumed AEC Charges	71
XXI	Fuel Cycle Cost	71

SECTION I

INTRODUCTION

The designs of two compact, unattended nuclear power plants are pursued, a 100-kilowatt(e) plant utilizing Stirling cycle energy conversion and a 10-kilowatt(e) direct conduction-cooled nuclear thermoelectric power plant. Each power plant utilizes hydrogen diffusion (H-Rho) reactivity control. Because systems may be viewed independently, the report is divided into two sections. Each section contains a general plant description followed by the supporting design analyses.

Although both systems are derived from earlier work on the Terrestrial Unattended Reactor Power System (TURPS)[3], there has been a considerable amount of design change. The basic control mechanism is the same but the fuel form, hydrogen containment, coolant and energy conversion configurations have been modified. The many innovations applied have yielded plants that are particularly suited to the power levels selected, are lower in cost and require less developmental effort than the TURPS.

This page intentionally left blank.

SECTION II

H-RHO REACTOR-STIRLING POWER PLANT

A unique compatibility is evidenced by the coupling of an H-Rho controlled reactor with a Stirling engine in that the reactor coolant can be used directly as the heat engine working fluid. High efficiency at modest temperature is afforded by an engine based on the Stirling thermodynamic cycle, which, with the addition of regeneration, theoretically can attain the efficiency of a Carnot cycle. In addition, the preferred working fluids, helium and hydrogen, have low activation cross sections and are compatible with common reactor materials, thereby facilitating fabrication and operation of the power plant.

The Stirling cycle requires displacement piston machinery in expansion and compression chambers to extract mechanical energy and supply pumping power. The fluid flow is cyclic, but oscillatory as contrasted with the steady, continuous flow of a Brayton cycle. However, because of the thermal inertia of the reactor, the core temperatures do not fluctuate significantly.

Various mechanisms have been used to create the cyclic gas pressure and volume displacement. The rhombic drive device[1] has been quite popular, but recently studies performed at General Motors Research Laboratories suggest a swashplate mechanism[2] which yields greater simplicity and compaction. The design presented in this report incorporates a four-cylinder swashplate engine to create a compact, coaxial arrangement of reactor, engine and electric generator.

The reactor fuel arrangement has also been simplified. A continuous fuel body penetrated by separately pressurized coolant tubes is used. The advantages of such an approach are manifold, the most important being fabrication simplicity, relative ease of hydrogen containment, and reduced structural requirements. The relatively high pressure of the Stirling engine working fluid (≈1500 psi) is readily contained in small diameter coolant tubes while the low gas pressure of the H-Rho control system allows a relatively light core vessel. Hydrogen leakage from the core vessel is limited by the vessel wall thickness plus the use of a diffusion barrier such as enamelling. Hydrogen leakage from the fuel into the

gas working fluid is allowed to reach an equilibrium condition at a very small concentration (~1 atmosphere out of 100 atmospheres).

The H-Rho Stirling power plant offers fabricational simplicity, a high efficiency and inherent safety. This report presents the design of a 100-kilowatt(e) system which takes advantage of these characteristics to yield a relatively inexpensive, compact power generator.

1. System Characteristics

Combining H-Rho reactor control with Stirling engine conversion of thermal to mechanical energy results in a system that has many desirable features that must be considered in power generation. Compactness, low weight and minimum maintenance at small cost are possible with components that are the result of technological advance. The following contains a brief discussion of the significant characteristics of the plant. These are also presented in concise form in table I and figures 1 and 2.

Because of high conversion efficiency and forced coolant (helium) flow, a small core with a low fuel loading yields the energy output desired. In addition, the use of a single continuous fuel body avoids the complexities involved when using numerous fuel elements and facilitates hydrogen and fission product retention. The relatively high thermal conductivity of the fuel matrix alloy results in only small temperature rises between the cooling passages. These factors, together with simple means of construction and with the automatic fail-safe attributes of H-Rho control, yield a low cost, very reliable reactor.

Using the Stirling engine working fluid (helium) directly as the reactor coolant necessitates shielded separation of the core from the engine. However, the design simplicity afforded by avoiding an intermediate coolant loop is attractive, and the engine design can readily accommodate the increased working fluid volume without excessive losses in efficiency. To accomplish the energy conversion, a four-cylinder swashplate engine is selected. Consultation with General Motors Research Laboratories[2] revealed that the swashplate drive is more compact and mechanically simpler than rhombic drive devices. Further, it is felt that an 1800-rpm engine, devoid of conventional fuel combustion complexities, can be built as a sealed unit and operated for long periods without maintenance.

Table I

STIRLING CYCLE TURPS CONCEPTUAL DESIGN CHARACTERISTICS

System	
Thermal power (kw(t))	400
Electrical power output (kw(e))	100 net
Net efficiency (%)	25
Operating life (yr)	5 at 400 kW(t)
Reactor	
Core diameter (in.)	14.2
Core height (in.)	14.2
Coolant	Helium
Coolant tubes (No.)	224
Coolant tube inner diameter (in.)	0.177
Free flow area ($in.^2$)	5.5
Fuel temperature (°F)	
Average	1410
Maximum	1570
U-235 loading (kg)	6.8
U content of U-Zr alloy (wt %)	5
U-Zr loading, core U-ZrH_x (kg)	145
Zr loading, reservoir ZrH_x (kg)	135
Initial X in U-ZrH_x	1.45
Initial X in ZrH_x	1.60
Total burnup U-235 (kg)	0.7
Density (% of theoretical)	
Core	80
Reservoir	80
Thorium reflector thickness (in.)	2.0
Stirling Engine	
Type	4 cylinder, swashplate drive
Working fluid	Helium
Mean working pressure (psi)	1560
Mean coolant tube wall temperature (° F)	1300
Efficiency (%)	30

Table I (cont'd)

Speed (rpm)	1800
Speed stability, steady-state (%)	±1/3
Transient speed surge--70 to 100%; and 100 to 70% load change (%)	±1/2
Time for complete recovery from transient (sec)	3
Generator	
Type	Brushless exciter, static voltage regulator
Output power (kW)	100
Output (volts)	120 and 208 60 Hz, 3-phase, 4-wire
Operating speed (rpm)	1800
Conversion efficiency (%)	90
Output power stability (%)	
Steady-state	
Voltage	±1/2
Frequency	±1/2
Transient	
Voltage	±1/2
Frequency	±1/2
Blower	
Brake output (hp)	15
Air flow (lb/hr)	36,000
Nominal air temperature (°F)	
Inlet	70
Outlet	170
Fan and motor efficiency (%)	77
Net auxiliary power (kW)	14.5

Table I (cont'd)

Weight Estimate (lb)

Reactor compartment (Fig. 2)	2610
Stirling engine	800
Generator	1350
Blower	250
Total	5010

The excellent speed governing ability of pressure-regulation control of the Stirling engine enables use of a standard rotating generator for production of 60 hertz electrical power. With the load-following capabilities of heat source and prime mover, a brushless exciter machine with static voltage regulation can provide very precise reliable power, with maximum voltage and frequency variations of only $\pm$ 1/2 percent.

Although water cooling for the Stirling engine would allow efficient heat removal at negligible power consumption, the elimination of such an extra cooling loop at the expense of about 15 kilowatts pumping power for forced air cooling is selected for this plant. Thus, a blower is attached to the generator shaft to provide cooling for the Stirling engine as well as for other components such as the generator, shielding and hydrogen reservoir.

It is apparent from the tabulated data and accompanying drawings that the power plant is compact and low in cost. Its total weight, including engine access shielding, is only 5010 pounds. This is about 60 percent lighter than the previous thermoelectric conversion 100-kilowatt(e) TURPS[3] without relocatable shielding. Moreover, at an estimated capital cost of $134,500 and with fuel cycle costs of 2.3 mills/kw-hr (excluding use and burnup charge), it is economically attractive for unattended, reliable power.

A relocation capability was omitted when this H-Rho-Stirling power plant concept was evolved. Although the basic plant weight allows it to be air transportable, inclusion of shielding for shipping after any significant operation imposes weight and cost penalties which are considered excessive for a

BLANK PAGE

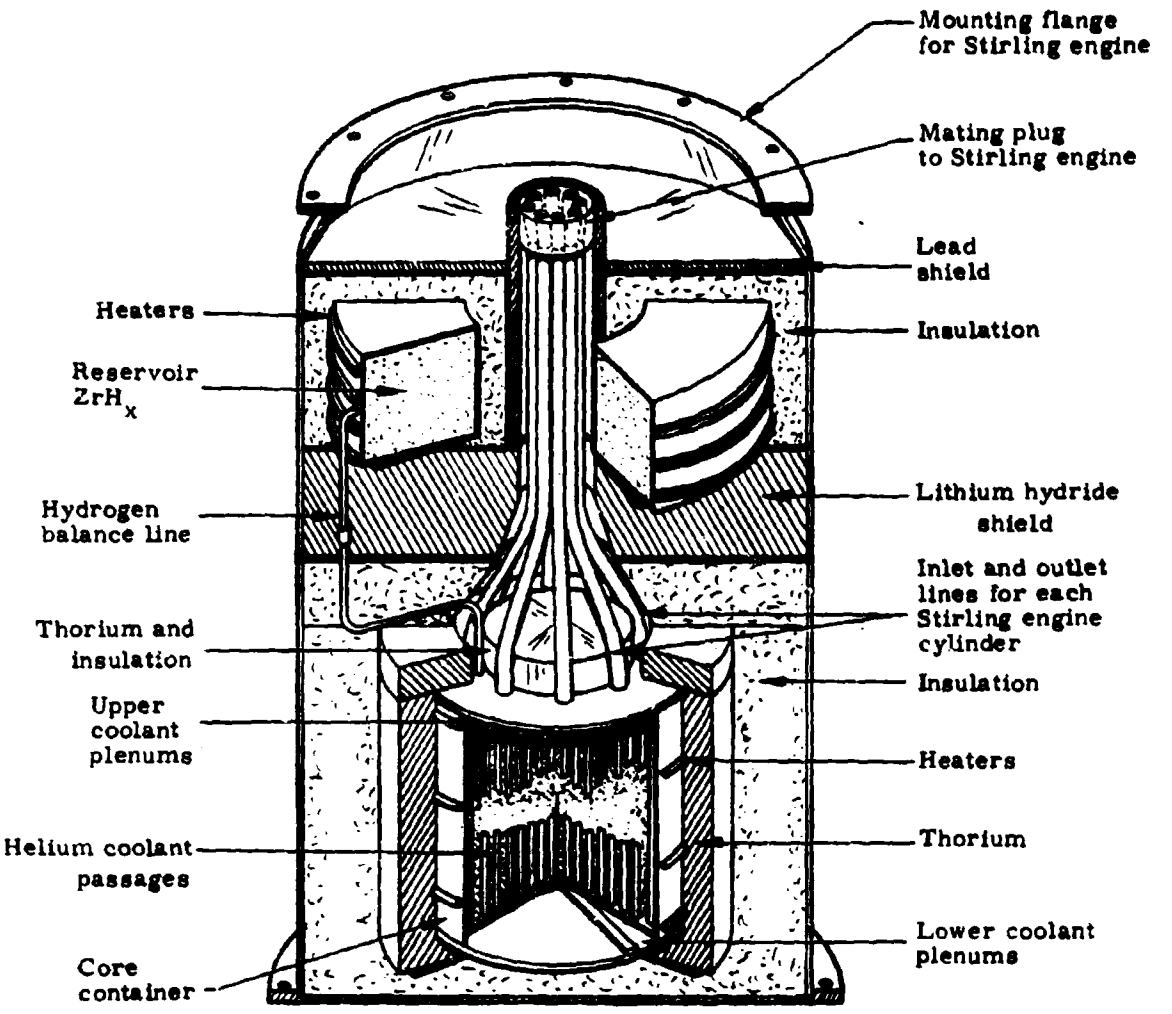

Figure 2. H-Rho Reactor Compartment for Stirling Engine System

system designed primarily for long-term, unattended operation. Thus, indigenous material and structural concrete, together with polyethylene, are considered separate facility requirements. This allows for providing shielding according to site requirements. For plant removal, the reactor compartment will be raised into a specially provided shipping cask.

2. Analysis

a. Nuclear Analysis

The nuclear characteristics of the Stirling cycle power system differ considerably from the original TURPS concept because higher conversion efficiency results in lower thermal power, and the use of a forced flow gas coolant permits reduced coolant volume. In addition, a modified fuel arrangement, consisting of a continuous body penetrated by separately pressurized coolant tubes, makes possible a more fully utilized core volume by facilitating hydrogen and fission product containment.

The nuclear characteristics of the core were evaluated by performing initial reactivity and depletion studies for suitable ranges of important parameters such as core size and fuel loading. Information generated in previous TURPS work[3], together with preliminary thermal-hydraulic analysis, enabled specifications for fuel matrix density, reflector material and thickness, coolant volume and cladding volume to be established. The values of these fixed parameters are listed in table II. It should be noted that the coolant and cladding volumes are typical values for a range of Stirling engine designs and thereby represent a good estimate of the reference design values presented. In addition, the neutron cross section of stainless steel are sufficiently close to Hastelloy that interchanging of these materials has negligible effect on nuclear characteristics. It should be noted that the coolant gas exerts negligible reactivity effect, whether it be helium or hydrogen, at any pressure typical of Stirling engine operation.

Table II

FIXED PARAMETERS FOR NUCLEAR ANALYSIS

Core geometry	Right circular cylinder with L/D = 1.0
Reflector	2.0 in. thick thorium
Cladding material	Stainless steel
Coolant	99% He + 1% H_2
Volume fraction	
Fuel	0.900
Cladding	0.025
Coolant	0.075
Power level (kW(t))	400
Core life (yr)	5 at 400 kW (t)

(1) Methods

The analysis techniques used in the nuclear studies are described in detail in reference (3). All cross sections and computer programs used in the reactivity-lifetime studies were identical to those reported in this reference.

(2) Results

(a) Initial reactivity: Initial reactivity studies of the relationship between fuel loading and core diameter indicate that significant reductions from the previous TURPS design[3] can be achieved. Figure 3 illustrates that for a 10 weight percent uranium (93.2 percent U-235) fuel matrix of 80% density (original TURPS specification), an active core diameter of about 13.3 inches is sufficient for five-year operation. Moreover, reducing the uranium content to five weight percent yields a core of only 14.2 inches in diameter with a significant reduction in fuel loading from 11.8 to 6.8 kilograms U-235. This tradeoff between fuel loading and core volume cannot be extended much below a five weight percent matrix for at this point the volume increases rapidly and fuel loading changes little.

(b) Depletion and control: In order to evaluate the H-Rho control system capability for a small core of lower fuel density than the original TURPS reactor design, the core reactivity variation with hydrogen content was

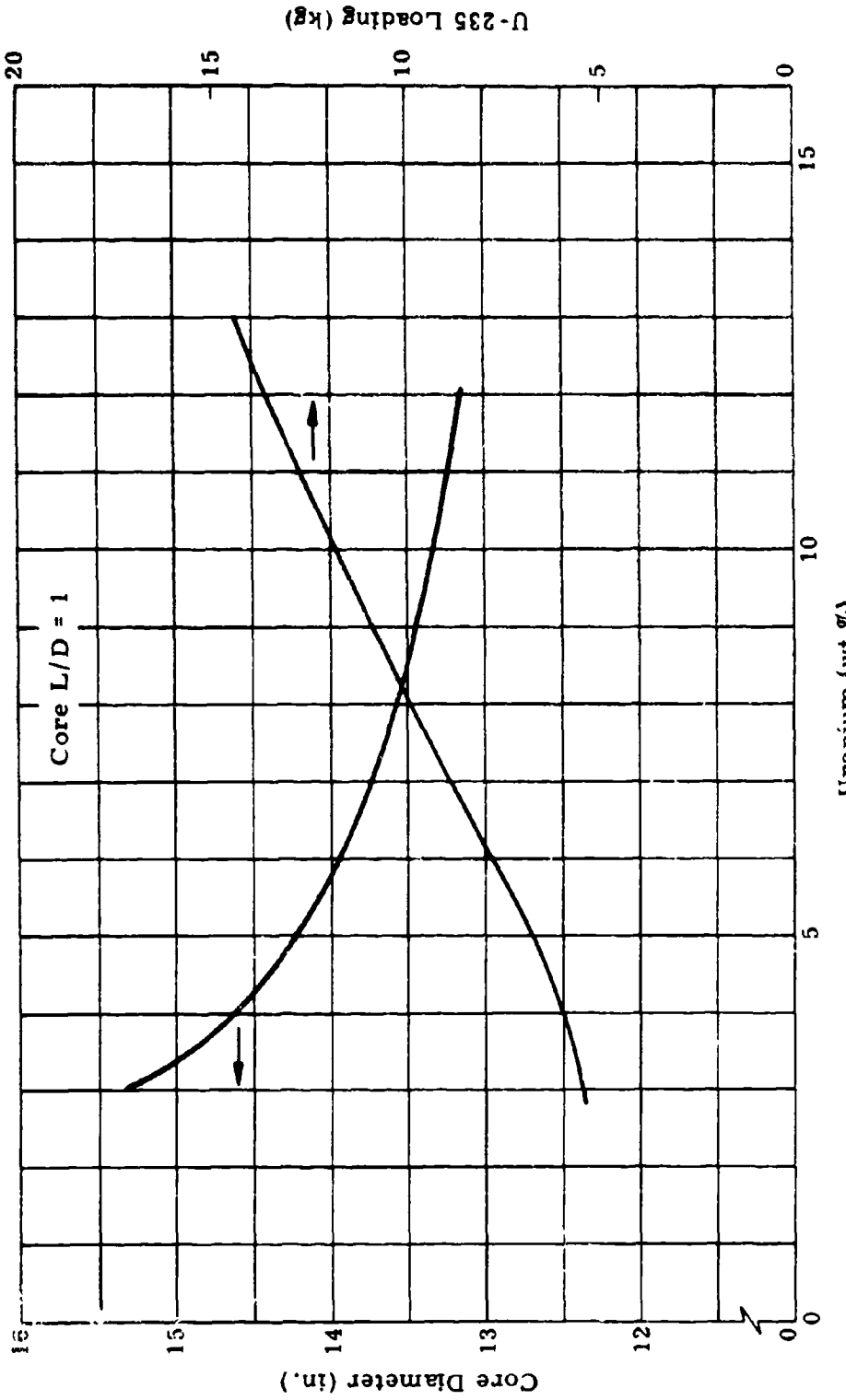

Figure 3. Core Diameter and Fuel Loading Variation with Fuel Matrix Weight Percent Uranium for 5-Year Operation at 400 Kilowatts(t)

evaluated and compared with the results of depletion calculations. Figure 4 shows the reactivity-hydrogen density relationship for a five weight percent core, while the reactivity inventory for the same core is listed in table III. It is apparent that ample control is available by allowing an X (of ZrHx) variation from 1.45 to 1.85.

Table III

REACTIVITY INVENTORY AND CONTROL MARGIN FOR A FIVE-WEIGHT PERCENT CORE

Quantity	% $\Delta\rho$
Shutdown to cold critical	1.50
Cold critical to hot full power	2.95
Equilibrium fission products	2.00
Fuel burnup	4.50
Hydrogen redistribution	-0.40
Total control required	10.55

Available control for X from 1.45 to 1.85 (figure 4) = 13.35%

Control margin 13.35 - 10.55 = 2.8%

It should be noted that the hydrogen worth increases slightly for higher fuel density cores while the activity requirements are reduced because of smaller fractional fuel depletion. For example, the control margin for a 10 weight percent core is increased to 3.8T $\Delta\rho$ for an X variation of 1.45 to 1.85.

These control quantities are for core designs containing no burnable poison. The incorporation of burnable poison in the fuel matrix substantially reduces control requirements. Thus, if operational advantage is gained by reducing the hydrogen-to-zirconium ratio variation, the use of burnable poison such as boron will readily accommodate such design modification.

(c) Power distribution: Power peaking in the smaller core (14.2-inch diameters compared to 18.5 inches for the original TURPS) is increased because of greater neutron leakage. Radial and axial flux peaking factors of 1.45 and 1.25, respectively, are present in the 14.2-inch core.

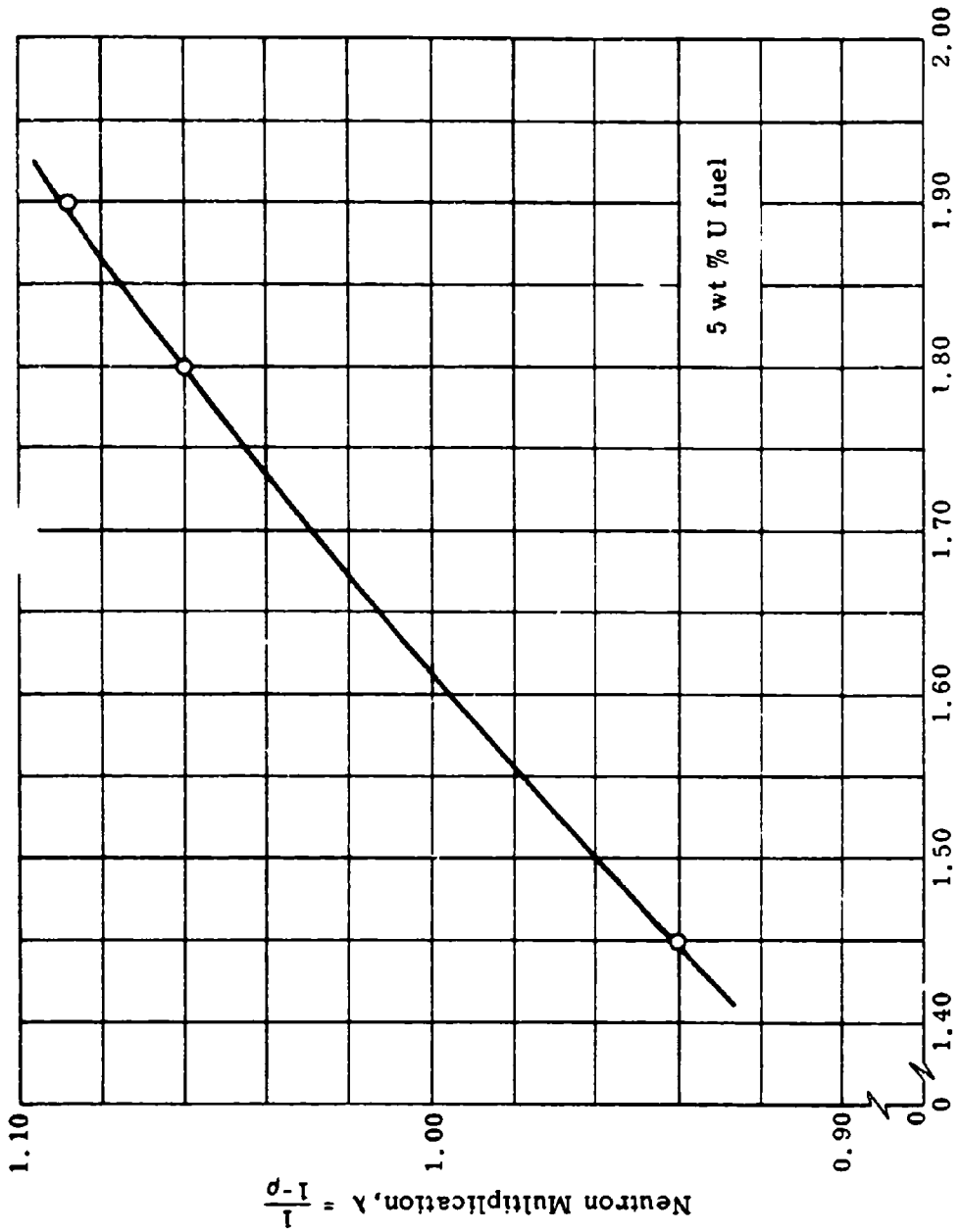

Figure 4. Relationship Between Fuel Region Thickness and Outer Diameter for 10-Year Operation at 200 Kilowatts(t)

Thus, an overall peaking factor of 1.82 is obtained in the thermal-hydraulics analysis.

(d) Shielding: Because of the limited estimated life of the first generation Stirling engine (≈10,000 hr) provision for replacement of the engine is made by activation shielding of components requiring accessibility. In order to prevent excessive activation of materials and to provide shutdown gamma shielding, a 12-inch thick shield is placed between the reactor and engine-generator compartments. The shield will consist of a 9.75-inch thickness of lithium hydride backed by 0.25 inch of boral and 2.0 inches of lead. This will enable accessibility to the engine while the reactor is shut down with gamma dose rates less than 200 mr/hr.

For operational shielding considerations, the activation shield of hydride and boral or the equivalent in other material such as concrete, must completely surround the reactor to prevent ground activation. The remainder of the neutron and gamma shielding required will be provided by indigenous earth as in the original TURPS design.

(3) Summary

The compact arrangement of fuel and coolant material, together with reduced thermal power requirements, enables a small core of low fuel density for the Stirling cycle conversion system. The 14.2-inch diameter and 6.8-kilogram U-235 design point values yield a core whose volume and fuel loading are less than one-half those of the original TURPS design. This reduction in size is accompanied by a decrease in shielding with consequent savings in plant weight. A small increase in power peaking is readily accommodated by alteration of the coolant channel configuration.

b. Steady-State Thermal-Hydraulic Analysis

(1) Method

Since the Stirling engine working fluid, helium, is used directly as the reactor coolant, the allowable volume, pressure, and flow rate of the coolant is strongly dependent upon the engine design characteristics. Therefore, the thermal-hydraulic analyses were preceded by preliminary studies of

Stirling engine performance. The effects of helium temperature, pressure and dead space upon engine specific output (power per unit displaced volume) and efficiency were evaluated for a wide range of engine displacements. A lumped linear system model[4] describing the expansion chamber, heater, regenerator, cooling chamber and compression chamber was used.

With these initial estimates of engine characteristics, detailed thermal-hydraulic core analyses were made for a broad range of parameters. Average and maximum fuel temperatures were evaluated for several values of working fluid pressure, temperature and in-core volume as well as overall system efficiency, dimensions and number of reactor coolant passages. Reactor core power peaking was also carried as a parameter, with an overall flux peak range of 1.5 to 2.0.

(2) Results

The preliminary Stirling cycle studies showed that for reasonably small (~200 cubic inches) engine displacements (swept volume of displacer and power piston), an overall efficiency of about 35% could be obtained for dead (unswept gas volume) volumes of 60 to 100 cubic inches and helium temperatures of approximately 1150°F at 1500 psi pressure. Further, it was estimated that about 20 to 40 cubic inches of the dead space would be available for reactor coolant volume. Thus, the ranges of thermal power and coolant conditions were established.

Initial thermal-hydraulic studies revealed that fuel temperature is not a strong function of coolant pressure drop above 10 psi. Figure 5 illustrates the behavior for a representative core configuration. Since 10 psi is quite tolerable from the engine efficiency point of view, the value was selected for more detailed investigations of coolant configuration.

The effect of core coolant volume on average fuel temperature for conversion efficiencies from 25 to 40 percent (300 to 480 kilowatts(t)) is shown in figure 6 for a core with 200 coolant channels. It is apparent that beyond about 50 cubic inches little average fuel temperature reduction is achieved by increasing coolant volume (recall that the pressure drop is held constant at 10 psi).

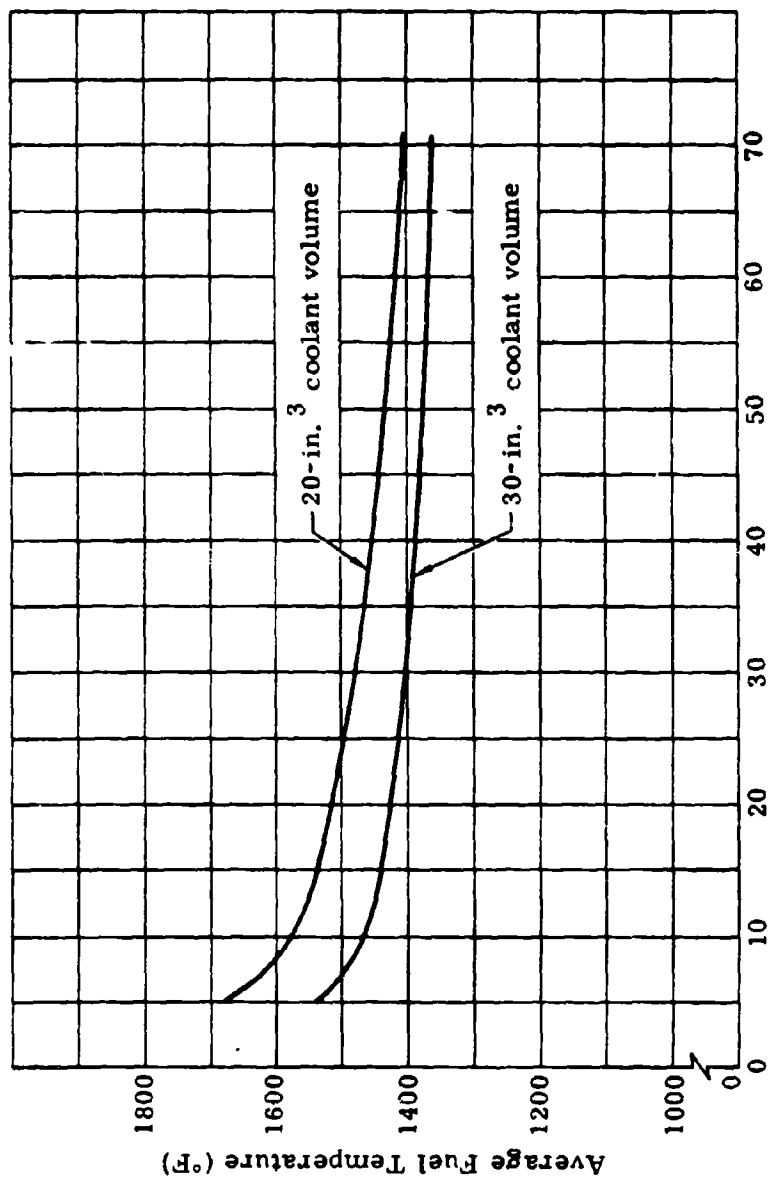

Figure 5. Effect of Core Coolant Pressure Drop on Fuel Temperature for Core Power Level of 500 Kilowatts(t)

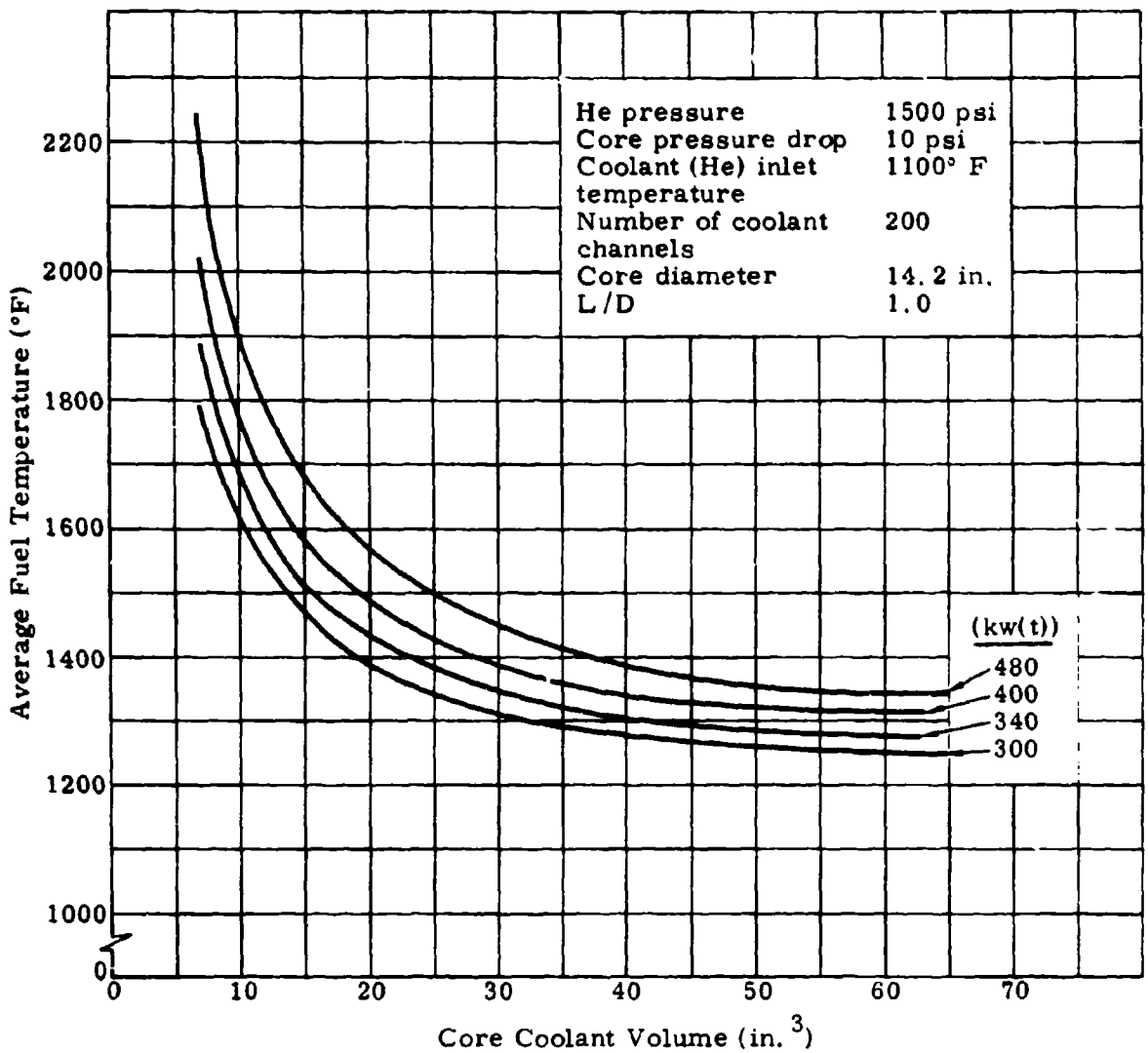

Figure 6. Effect of Core Coolant Volume on Average Fuel Temperature

By increasing the number of coolant passages, the heat paths through the fuel matrix are shortened, thereby reducing the fuel temperature. This effect is shown in figure 7 where average fuel temperature is graphed against the number of coolant passages, with coolant volume and coolant tube diameter as parameters. The obvious fact that increasing the number of coolant passages and the total coolant volume yields the steepest ratio of reduction in fuel temperature is illustrated by the constant coolant tube diameter lines.

Because of gross radial and axial power distribution nonuniformity, higher fuel temperatures will exist near the core center. By using radial and axial peaking factors of 1.45 and 1.25, respectively, (obtained from the nuclear analysis), the results of figure 8 are obtained. To keep the fuel matrix entirely in the δ-phase (for 0.9 atmosphere H_2 pressure design conditions) more than 200 coolant passages are required for an in-core coolant volume of 42 cubic inches, and the number is reduced to about 150 for a coolant volume of 78 cubic inches.

The maximum fuel temperature in figure 8 is for a helium inlet of 1100° F. In order to gain increased efficiency, the selected engine design utilizes a helium inlet temperature of about 1200° F that corresponds to an average coolant wall temperature of 1300° F. For these conditions, 224 coolant tubes of 0.177-inch ID yields a maximum fuel temperature of 1570° F.

It is important to note that these studies were performed for uniform distribution of coolant channels throughout the core. By radial and axial variations of spacing (such as by curving of the coolant tubes) much more uniform temperature profiles may be obtained, thereby enabling raising of average temperatures to yield increased conversion efficiency, or providing increased thermal design margin.

(3) Summary

It is apparent that adequate heat transfer capability is provided by direct use of the Stirling engine working fluid, helium, as the reactor coolant. By using 200 to 250 coolant passages of approximately 3/16-inch ID, core

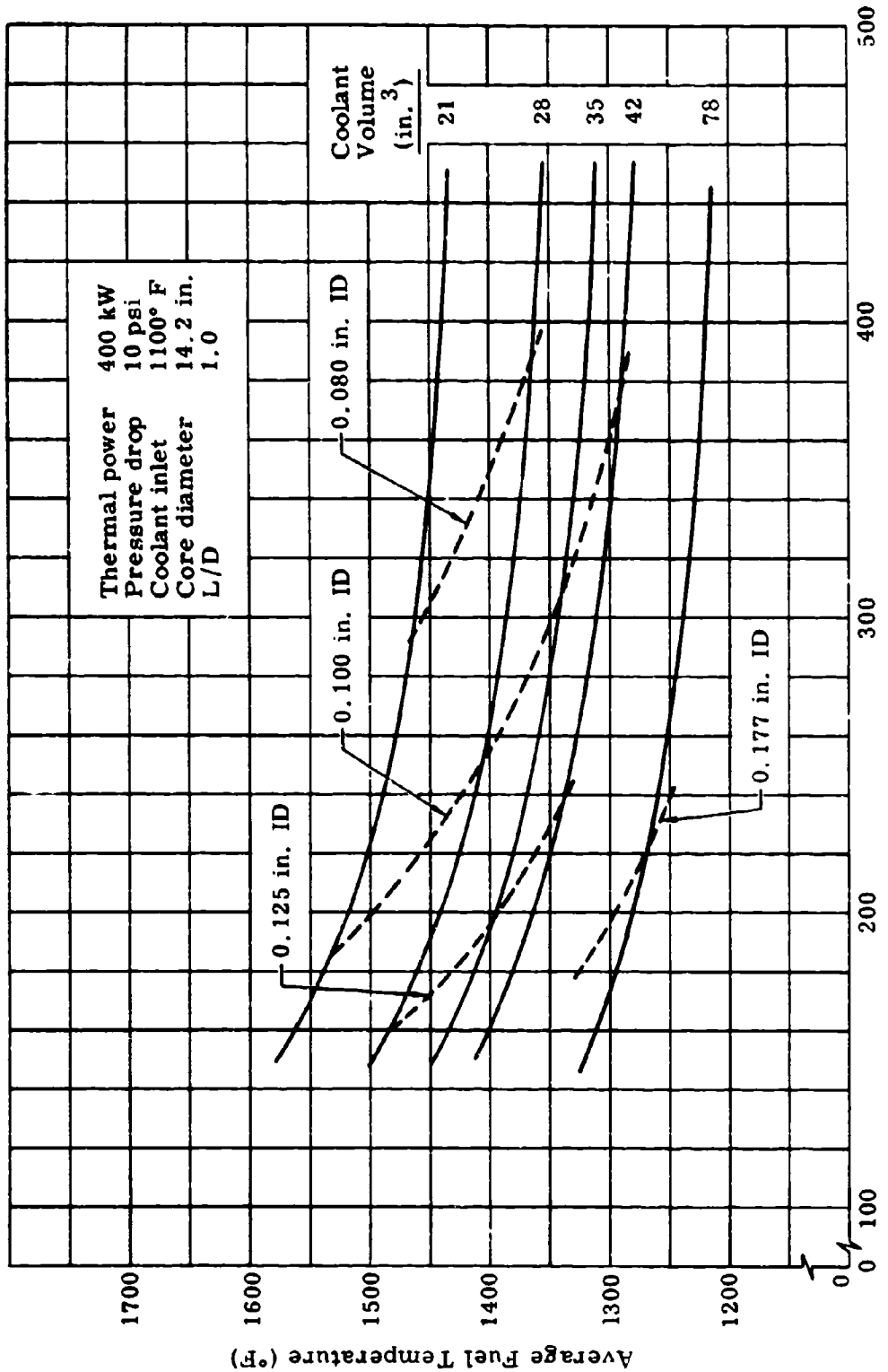

Figure 7. Effect of Number of Coolant Tubes on Average Fuel Temperature

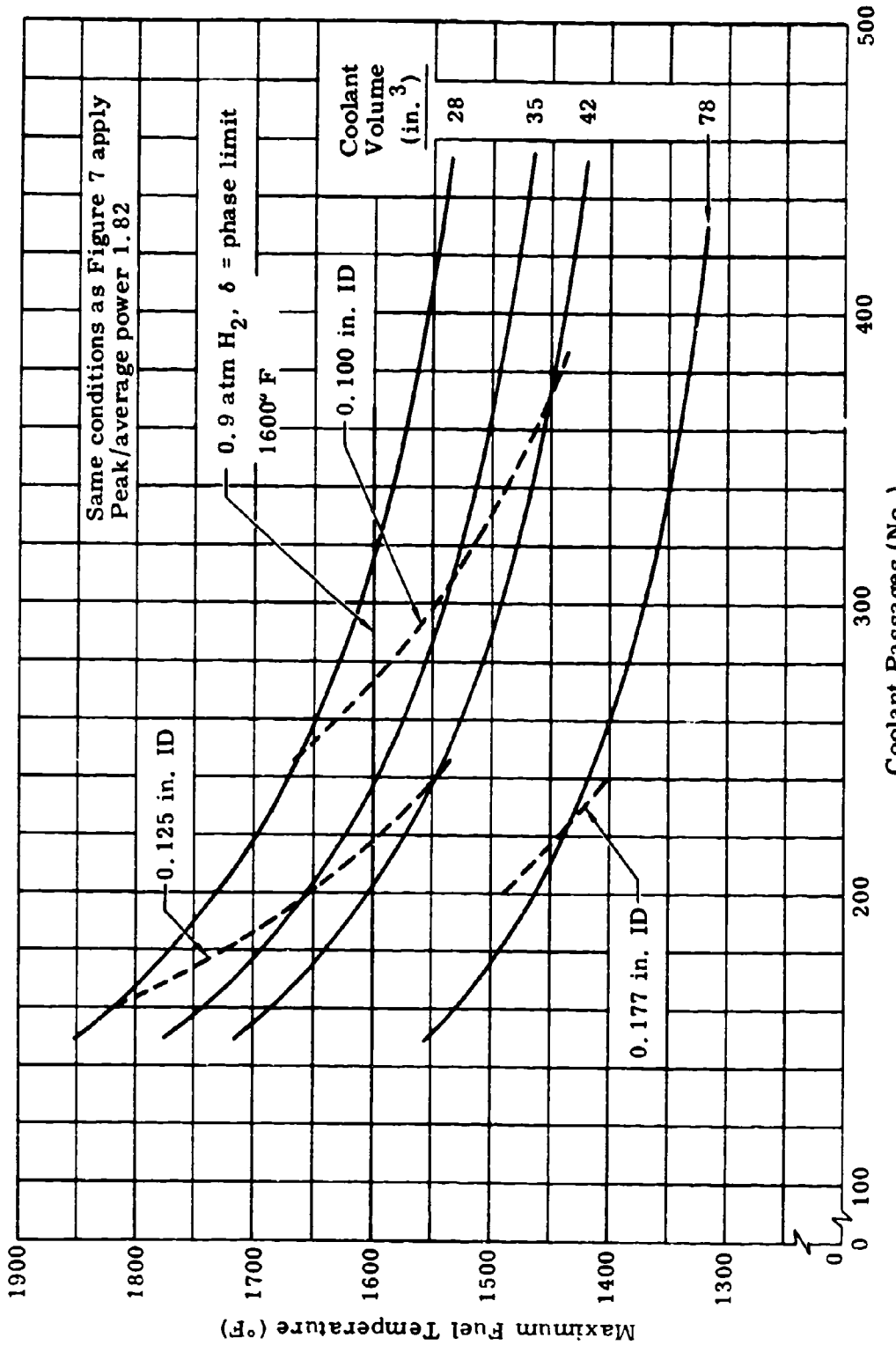

Figure 8. Effect of Number of Coolant Tubes on Maximum Fuel Temperature

temperatures can be kept within the δ-phase limit of 1600° F at 0.9 atmosphere hydrogen pressure. Moreover, the coolant flow rate is sufficiently low through these tubes so that only a small pressure drop is experienced (10 psi). Thus, a reactor core 14.2 inches in diameter and 14.2 inches long can operate readily at 400 kilowatts(t) to yield a mechanical output of 120 kilowatts from a compact Stirling engine design.

c. Dynamics Analysis

(1) General

The dynamic response characteristics of the reactor-engine-generator were investigated to devise an integrated power supply which could meet desired specifications, yet be a simple reliable system. At first, a variable speed engine and generator were considered because of uncertainty in the capabilities of Stirling engine speed governing and a desire to minimize control functions. However, it was learned from the General Motors Research Laboratories[2] that a proven pressure-regulating governing method exists which acts rapidly and exhibits high inherent reliability and speed stability. Typical observed performance is as follows:

	Speed Change (%)
Steady load	± 1/3
No load to full load droop	1/4
Transient (no flywheel)	
Maximum surge (full load change)	4
Recovery (for full load)	6 sec

To relate such behavior to the Stirling engine-generator combination under consideration for the specified load changes of from 70 to 100 percent and 100 to 70 percent power, the following detailed explanation is offered.

(a) Load increase: At the onset of load increase, the engine speed decreases at a rate determined by the system inertia and magnitude of the load change. However, the pressure regulator acts as soon as the 1/3

percent limit is reached, and within 0.1 second[2] the pressure reaches a value enabling the engine to supply the new power requirement fully. For a load change from 70 to 100 kilowatts, the inertia of the generator (60 lb-ft^2) and an additional 180-pound flywheel will limit the maximum speed change (surge) to 1/2 percent. After this maximum excursion the governor continues to adjust pressure in response to the speed and to whatever changes occur in heater or cooler temperatures. During return to the $\pm$ 1/3 percent range, thermal load on the reactor and engine output will remain equal to the electrical load demand.

(b) Load decrease: Upon load decrease, engine speed will rise, but when the 1/3 percent limit is reached, a governor-actuated by-pass valve reduces output torque despite the high pressure, and a compressor transfers the working fluid (helium) from the engine to a reservoir. The response is virtually immediate, so that the flywheeled performance is well below a speed surge of 0.5 percent for the load decrease condition.

The analysis of the dynamic response of the coupled core-Stirling engine was greatly simplified by the effective control system. Engine output follows the load demand closely. Consequently, the electrical output response to load demands is determined by the generator regulation system characteristics in conjunction with the Stirling engine rpm control system.

In view of this performance, the dynamics analysis of a coupled core-Stirling engine system assumed no lag between the electrical load demand change and the thermal load on the core coolant (also the engine working fluid). This time lag is negligible compared to the thermal time constant because of the core heat capacity. The effects of the heat capacities of coolant and core were included in the model, as was the pressure effect on the heat transfer coefficient between the core and coolant. The heat flow from core to coolant was related to the respective average temperatures. The H-Rho control system was assumed to operate at constant pressure (i.e., a large hydride donor reservoir), and the time lags resulting from hydrogen transport and diffusion in the hydride beds were neglected. Fuel forms for which these assumptions are valid for operating condition transients have

already been tested[5]. The reactivity effect of hydrogen migration into or out of the core was coupled to the core thermal power level via a neutron kinetics model utilizing one averaged group of delayed neutron precursors. The set of coupled differential equations describing this model was integrated by the use of an IBM-360 digital computer with Digital Simulation Language (DSL)[6].

(2) Results

The results of the use of this model for step load changes of 100 to 70 kilowatts(e) and 70 to 100 kilowatts(e) are shown in figures 9 and 10, respectively. The core power and fuel temperature are the major variables of interest. It is seen that the coolant temperature changes almost immediately, because of its small heat capacity, to provide the temperature difference necessary to remove the new thermal load from the core. Thereafter, the coolant temperature simply follows the fuel temperature.

For the load increment from 70 to 100 kilowatts(e), the core power rises from the initial steady-state value of 286 kilowatts(t) to a peak value of 439 kilowatts(t) 42 seconds after the step load change and stabilizes at the final steady-state value of 400 kilowatts(t) within three minutes. The fuel temperature overshoot on a load increase is very small, with a peak value only 1.2° F higher than the steady-state value, occurring at about 90 seconds after the load change.

For the load decrease, the power stabilization time is somewhat longer (~ 4 minutes). The fuel temperature rise is also larger with a peak 7.8° F higher than the steady-state average value. This occurs about 30 seconds after the transient initiation.

It is apparent that the H-Rho control system is able to provide a load-following capability with a small fuel temperature variation. Thus, the assumption of separability of engine response from core response is validated. This analysis illustrates the typical smooth stable behavior of H-Rho control. Well-damped response is observed for the design parameters selected.

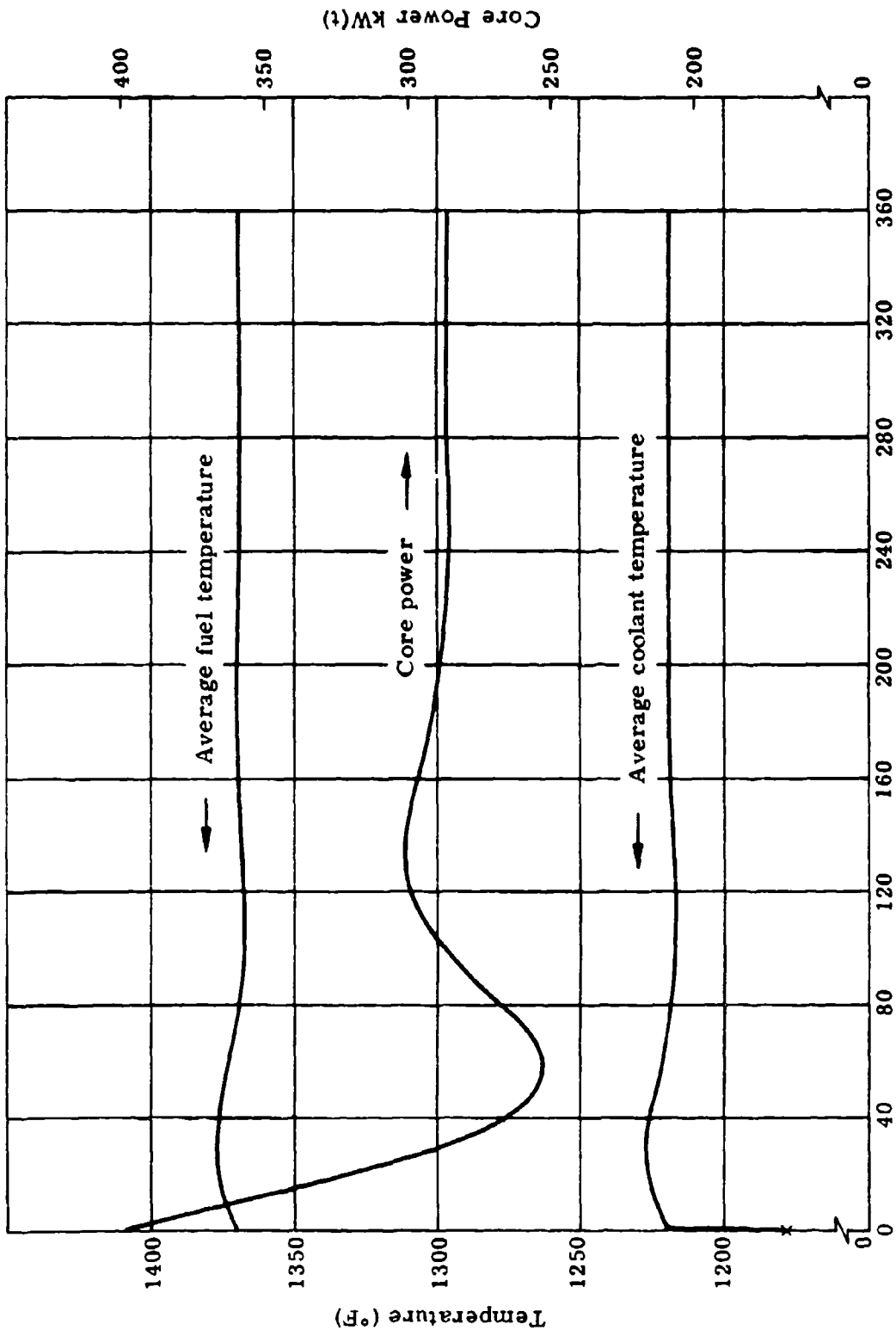

Figure 9. Response to Step Change in Electrical Load from 100 to 70 Kilowatts for Stirling Engine System

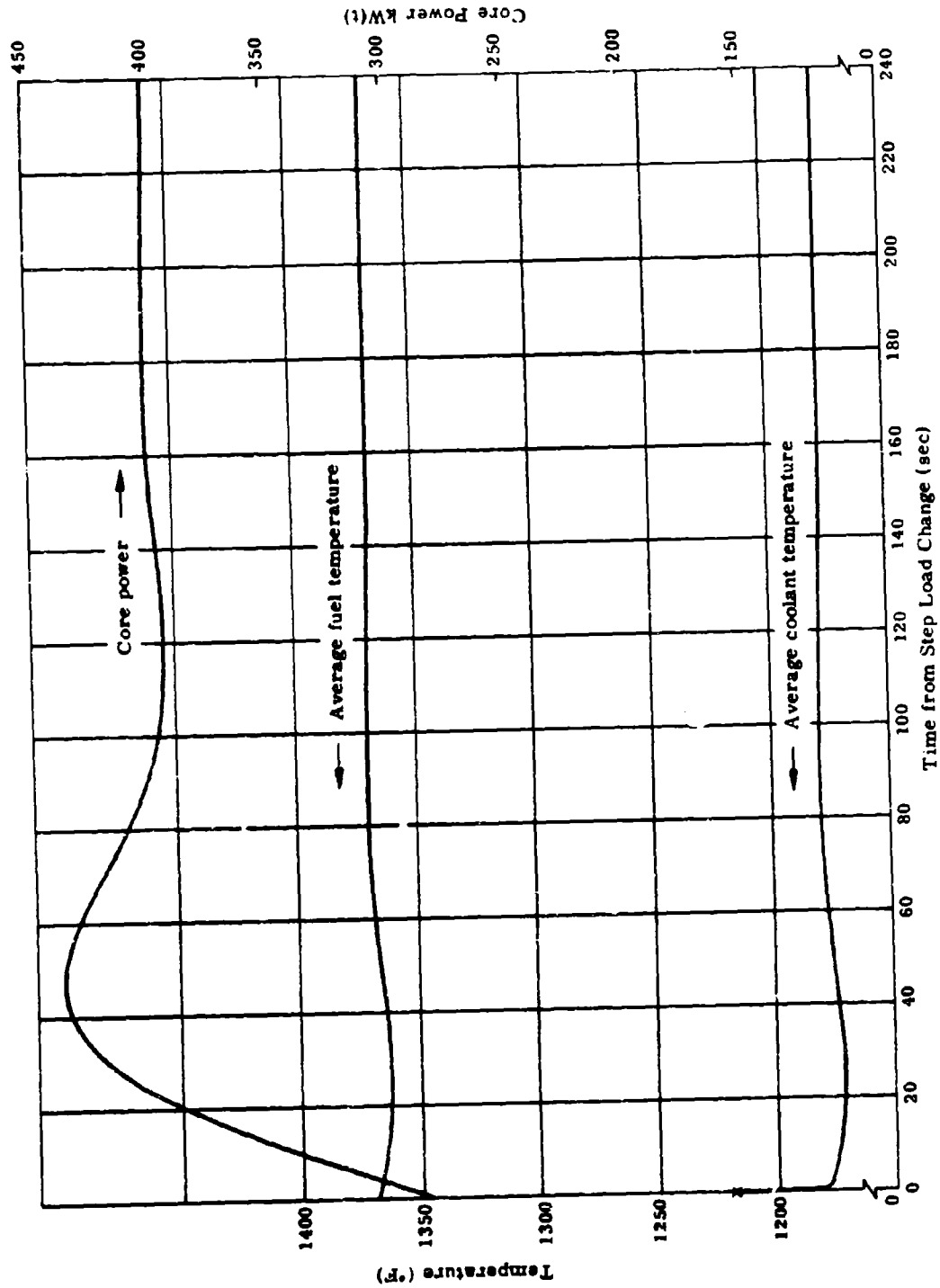

Figure 10. Response to Step Change in Electrical Load from 70 to 100 Kilowatts for Stirling Engine System

(3) Conclusions

The rapid response characteristics of the pressure-regulation method of Stirling engine control, aided by a flywheel, can supply a nearly constant driving speed (± 1/2 percent) to the electrical generator at all times during the steady-state and transient conditions studied. The ability of H-Rho control to provide a stable, load-following heat source ensures such response for any sequence of transients and during the entire operational life. Thus, the ability to furnish voltage within a 1/2 percent tolerance is a function solely of the system electrical characteristics, and adequate solid-state circuiting regulation means can be supplied to satisfy this small tolerance. Frequency control, of course, is automatically satisfied by the speed regulation.

d. Mechanical Design Configuration

As shown in figure 1, the power plant configuration consists of a stacked coaxial arrangement of reactor core, shielding, reservoir, engine, generator, and blower. The design of these components and proposed assembly procedures are directed toward obtaining a compact, easily fabricated plant, thereby enabling low construction costs. The features of each major component are discussed.

(1) Reactor compartment

As shown in figure 2, the fuel form is a continuous body permeable to hydrogen and penetrated by separately pressurized coolant tubes. This feature allows the core assembly to be initiated by welding the coolant tubes through a bottom plate and attaching the cylindrical core container wall to this plate. Unhydrided U-Zr alloy powder is then loaded into the container and compacted around the tubing. A top plate with the hydrogen passage line attached is then welded to the coolant tubes. This completes the fuel and hydrogen containment shell, leaving helium coolant passages through the fuel matrix.

Top and bottom helium distribution is provided by spider plates sandwiched between the core containment end plates and an outer plate. At the top, the

spider plate creates eight separate coolant regions, each of which is connected to eight helium lines connected to and penetrating the top outer plate. (An inlet and outlet line is required for each of the four Stirling engine cylinders.) At the bottom, the spider plate forms a four-coolant region plenum, each region connecting down flow and up flow paths through the core.

Final brazing of the sandwich plenum and sintering of the fuel matrix may be carried out in a single furnace operation. Initial hydriding of the fuel matrix to a significant, but safe, level can also be performed at this time.

Insertion of the completed reactor assembly into the thorium reflector and insulation regions contained in an outer aluminum structure completes the assembly of the lower half of the reactor compartment. A wrap-around heater is embedded in the thorium reflector to serve as a temperature raising means for starting the reactor.

The upper half of the reactor compartment is fabricated as a separate unit for subsequent connection. This region contains the Stirling engine activation shielding as well as the hydrogen reservoir. It is annular in shape with a central hole for the eight helium passages. Shielding in the center is provided by avoiding a straight-through route from the reactor core and the use of interspersed shielding material. Aside from those required for structural support, the principal connection between the upper and lower halves of the reactor compartment is the joining of the single hydrogen passage line.

(2) Stirling engine compartment

This section of the power plant contains all of the components of the Stirling engine including the regenerator and cooler together with provisions for disconnecting the helium lines from the reactor core. The reciprocating translational output of four engine cylinders is converted into rotational motion by a swashplate connection. This is a simpler, more compact arrangement than the rhombic drive used in past and current single cylinder

Stirling engines. The swashplate engine design was suggested by the General Motors Research Laboratories, and details of its construction are considered proprietary and not available for release at present. However, GM assures that models have been built, and the design and construction of a working engine is quite straightforward[2].

It is estimated that first-production Stirling engines will have a life of about 10,000 hours. At present, there are no parts which can prevent such attainment. Bearings are the hydrodynamic type and lack of contamination makes oil changing unnecessary. Seals have already demonstrated service lives in excess of one year, and piston rings can also be designed for such operation.

Subsequent development is expected to considerably extend engine life. It is anticipated that for second-round engines lifetimes will double, and eventual achievement of the five-year goal (~50,000 hours) depends upon the demand and amount of developmental funding available. It should be noted that the Stirling engine is more capable of being designed for very long life than an internal combustion engine because it can be developed into a hermetically sealed machine. The gas volumes are sealed from outside contamination and the crankcase can also be sealed separately. Thus, the Stirling engine can be compared to a modern refrigerator mechanism which is factory sealed and operable for many years without maintenance.

Because of the limited anticipated life of the first engines, provision for quick disconnection and connection of the engine from the reactor coolant lines is provided by sturdy mating flanges to which the helium lines from the engine and reactor are connected. The flanges are torque bolted together with the helium passage seals afforded by metal gaskets and O rings. The flanges can be disconnected by long-handled tools, and removal of the engine, generator, and blower as a unit permits access to the engine and its replacement.

(3) Generator compartment

The generator is a standard brushless exciter, 1800-rpm device which is direct connected to the Stirling engine. It is structurally mounted on the engine housing; installation and assembly are made as a unit with the engine.

Electrical voltage is regulated by static, solid-state electronics. This package may be mounted within the power-plant silo or above ground in the weather shielding housing to be located above the entrance and exit air ducts.

The five-year lifetime of this device matches that of the reactor and, hence, the same generator can be used with initial replacement Stirling engines. Since the engine must again be connected during such replacements, inspection and/or replacement of the generator could be made then if necessary.

(4) Blower

Heat transfer studies indicate that direct air cooling can provide the heat dump for the Stirling engine with the use of about 15 horsepower. Thus, sufficient engine output is provided to drive a blower mounted on the generator shaft. Cooling air flows from the blower to the generator and into th Stirling engine compartment. After leaving the engine, the heated air (170° F) flows down around the reservoir and intermediate shielding and between the core and outer duct through which the air rises and leaves via ducts in the stationary shielding. Thus, the blower provides all cooling air for the engine, generator, shielding and structural housings.

Although no detailed analysis has been performed, it is estimated that in the event of blower failure, sufficient natural circulation air flow will prevent an excessive temperature rise of the plant components. Failure of the blower will cause helium temperature to rise which, through the H-Rho control action, will cause reactor shutdown, and only a decay heat source will be present.

(5) Shielding

In order to facilitate access to the Stirling engine, the main shielding has been separated into two regions, a stationary shield and a small diameter removable shield. Figure 1 shows that the stationary shielding contains the entrance and exit air ducts which do not have to be removed during engine replacement. The removable shielding consists of reinforced concrete and borated polyethylene plugs that rest on the main stationary shielding.

Ground activation shielding is provided by an 18-inch thick concrete annulus. This material also serves as the main support structure which bears the entire weight of the plant.

e. Weight and Cost Estimate

(1) Weight estimate

The Stirling cycle reactor power system is quite compact and lightweight. Calculations of the reactor, engine, generator and blower components weights together with the required interconnecting structure, yields the values listed in table IV

Table IV

REACTOR-STIRLING SYSTEM WEIGHT

Component	Weight (lb)
Reactor compartment (Fig. 2)	2610
Stirling engine	800
Generator	1350
Blower	250
Total	5010

The reactor compartment includes the reactor core, helium piping, reservoir and engine activation shielding.

In addition to the active generator, additional shielding and structural material is required for plant installation. Approximately 17 cubic yards of concrete and 48 cubic feet of borated polyethylene is used for this purpose.

For plant removal, a shield plug weighing 4900 pounds must be raised. This weight includes the concrete, and polyethylene and the structural housing for the polyethylene.

(2) Cost estimate

(a) Plant capital cost: Plant costs are dependent upon rate and quantity of production. For this estimate, a production rate of 50 plants/yr is used. Reactors costs are derived from work performed previously[3] together with

additional factors that result from easier fabrication afforded by design modification. The Stirling engine cost estimate was obtained from reference 2. The generator and blower costs are catalog prices. Table V presents a summary of the cost data.

Table V

H-RHO REACTOR-STIRLING PLANT COST

Component	Labor ($)	Materials ($)	Total ($)
Reactor (excluding U-235 material costs)	31,900	14,600	46,500
Generator/blower	--	5,000	5,000
Shield plug, engine activation shielding and structure	29,400	9,500	38,900
Generator assembly	7,300	--	7,300
Stirling engine	--	20,000	20,000
Instrumentation	5,500	11,300	16,800
Totals	74,100	60,400	134,500

Despite the limited life of initial Stirling engines (~ 10,000 hours), the cost of only a single engine is included in this estimate. Since engine life will undoubtedly be increased as a result of continued development, it is considered inappropriate to penalize the total cost by assuming limited life for all engines. Replacement engines or engines installed in plants constructed after fabrication of the initial series will show at least twice the lifetime of the initial devices and the attainment of five-year service life is considered quite reasonable.

Since production facilities for the reactor do not exist, labor and overhead rates were assumed in arriving at the estimated costs. The following values which include overhead and profit, were used.

	($/hr)
Manufacturing labor	8.50
Engineering liaison labor	14.50

(3) Fuel-cycle cost: An estimate of fuel-cycle cost has been made based on the parameters given in tables VI through XI. The method used follows that described in TID-7025 (volume 4)[7] with these exceptions.

(a) All fabrication costs are reflected in the plant capital cost rather than in the fuel-cycle cost. This follows from the unique lifetime core that lasts the life of the plant.

(b) The usual use and burnup charges have been omitted. This is in accord with previous military practice while operating such nuclear plants as the PM-1 and PM-3A.

(c) No shipping charges are included for the assembled plant. These are charged against site operating expenses or plant capital cost. The results of the fuel cycle cost analysis are given in table XI. The initial loading is 7.3 kilograms of uranium and the total fuel-cycle cost is $9760 excluding burnup and use charges for fuel. The fuel portion of the power cost comes to 2.2 mills/kW-hr. Figure 11 shows the effect of the rate of core availability on fuel-cycle cost. The points plotted are optimum values. They represent minimum cost for reprocessing and charges while in storage awaiting accumulation of a batch. In reducing the availability rate from 200 to 20 plants per year, the fuel cycle costs are raised by about 24 percent.

Table VI

FUEL CYCLE PARAMETERS, SET BY DESIGN

Enrichment (%)	
Charged	93
Discharged	92
Thermal power level (kW(t))	400
Net power (kW(e))	100
Initial fuel loading (kg U-235)	6.8
Total fuel discharged (kg U-235)	6.1
Final plutonium inventory	Negligible

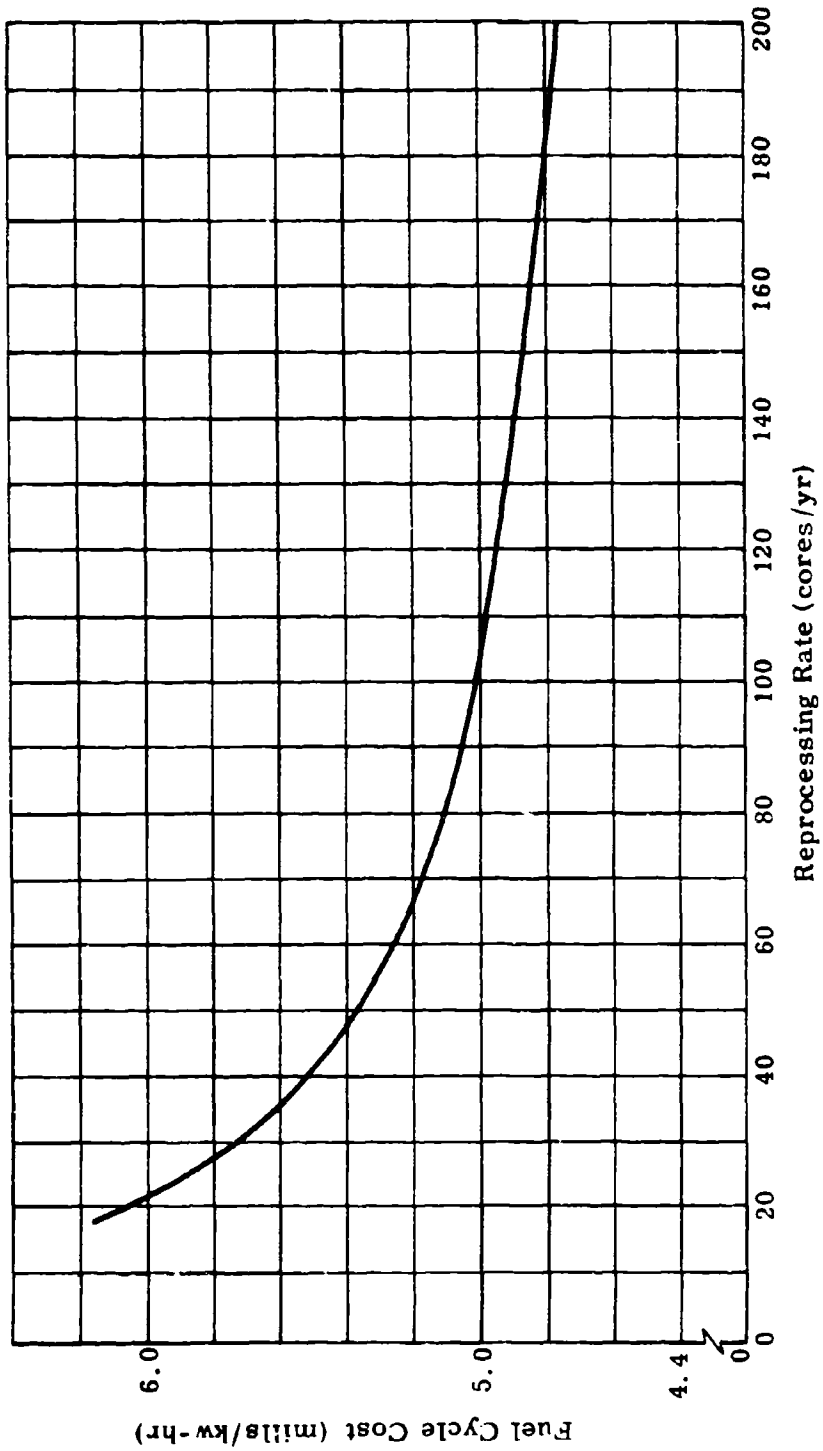

Figure 11. Effect of Reprocessing Availability Rate on Fuel Cycle Cost

Table VII

FUEL CYCLE PARAMETERS, TYPICAL VALUES SET BY INDUSTRY

Plant factor (%)	100
Shipping time-- AEC to fabricator (days)	20
Conversion plant throughput (kg/mo)	4000
Irrecoverable losses (%)	
Conversion	1
Fabrication	1
Recycle losses (%)	10
Fabrication time (days)	90

Table VIII

FUEL-CYCLE PARAMETERS, TYPICAL VALUES SET BY AEC

Minimum time before reprocessing (days)	120
Irrecoverable losses (%)	
Chemical separation	1
Conversion	0.3
Rates (kg/day)	
Chemical separation plant processing	44
Reconversion	150

Table IX

FUEL CYCLE PARAMETERS, ASSUMED INDUSTRIAL CHARGES

	($/kg U)
Conversion charges*	283
Shipping charges, AEC to fuel supplier	1.50

*Extrapolated from data given in TID-7025

Table X

FUEL CYCLE PARAMETERS,
ASSUMED AEC CHARGES

Prices ($/kg U)	
Uranium before use	10,385
Uranium after use	10,267
Conversion charges to UF_6	32.60
Shipping charge--reprocessor to AEC	1.00
Separations plant daily charge ($)*	21,000

*Extrapolation at rate of $500/yr from $17,000 given in TID-7025 (volume 4) for 1961

Table XI

FUEL CYCLE COST ($/kg U)

	Processing	Shipping	U Loss	Totals
Conversion and fabrication				
Transit to conversion		1.68		1.68
Conversion and fabrication*	283	1	208	491.
Reactor operation		**	****	0.0
Reprocessing				
Separation***	678	**	103	781
Conversion to UF_6***	28.60		33.80	62.40
Transit to AEC		0.90		0.90
				1336.98

*Fuel element manufacturing costs included in plant cost rather than fuel cycle because core lasts the lifetime of plant.

**Shipment of plant to and from site is charged to capital cost.

***Based on reprocessing availability rate of 200 plants/yr.

****Burnup cost waived.

SECTION III

DIRECT-CONDUCTION REACTOR THERMOELECTRIC POWER PLANT

Long term unattended power production is achieved by using mechanically passive control and energy generation methods of H-Rho and thermoelectrics. In addition, direct heat conduction eliminates the necessity for intermediate in-core coolant and provides a system simplicity which approaches that of a radioisotopic heat source, yet constitutes a safer and more economic power supply in the low kilowatt range. A representation of the reactor core, copper reflector-conductor and thermoelectric generator is shown in the following sketch.

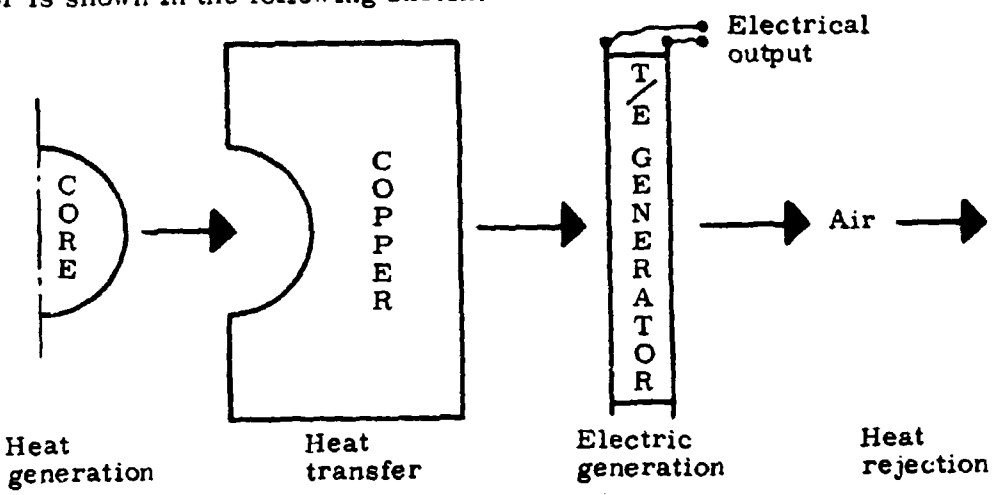

Although the power level presented in this report is 10 kilowatts(e), larger output can be achieved at the expense of increased plant size. Temperature rise through the copper and core regions can be limited by increasing the conduction area, thereby reducing heat flux. Similarly, heat rejection can be accommodated by natural circulation or forced air with a blower. Here, increased ducting size and cost associated with natural air flow must be weighed against blower energy cost.

The large thermal inertia of the copper conductor prevents rapid change of reactor core temperature and thereby aids safety by preventing large, rapid changes in core hydrogen content. Also, the copper forms a strong container which reduces the probability of core damage during accidental environment changes.

1. Plant Characteristics

Conceptual design characteristics of a 10-kilowatt(e) generator are presented in table X11. These data, together with the plant configuration depicted in figures 12 and 13 illustrate the simplicity of using a single fueled region having no penetration for coolant and no partitioning into fuel elements. Heat generated in the core region is conducted through the container vessel wall, across the intermediate heat-distributing copper conductor to the thermoelectric generator located at the assembly surface. Heat is rejected by forced-air flow at the finned, cold surface of the generator.

The copper conductor serves the reflector function for the reactor in addition to attenuating radiation and conducting heat. A minimum copper thickness of six inches is set such that immersion of the generator in water does not significantly affect core reactivity.

Hydrogen integrity of the system is provided by the outer core shell, the copper heat block, the reservoir container, the reservoir housing shell and the thermoelectric mounting shell. Each of these parts have brazed or welded closures. Copper is an effective high temperature barrier having a permeation rate to hydrogen of about 10^{-3} $cm^3/cm\text{-}hr\text{-}cm^2$ at 1000°F[9] and [10] and stainless steel is effective at low temperatures with a permeation rate of 10^{-4} $cm^3/cm\text{-}hr\text{-}cm^2$ at 300° F. The total hydrogen loss for 10 years operation will be less than 1%.

This conceptual design is based on the use of encapsulated high power density (HPD) thermoelectric elements. In size and shape these devices are similar to high current solid state rectifiers. Their fundamental advantages are inherent ruggedness, high heat and current handling capacity and the ability to operate in air. Thus, the generator is not hermetically sealed. Ordinary thermal insulation is used to limit heat loss, and the output junctions are readily accessible for measurement during checkout.

The underground installation shown in figure 12 indicates the operational shielding requirements. A surrounding concrete cylinder, 18 inches thick, prevents significant ground activation, while the main radiation shielding is provided vertically by five feet of borated polyethylene and two feet of concrete. The air ducting is mounted in the fixed shielding to facilitate plant removal through smaller shield plugs. Also, the blower is located outside of the main power plant in a separate compartment.

Table XII

CONDUCTION-COOLED REACTOR CONCEPTUAL DESIGN CHARACTERISTICS

System	
Thermal power (kW(t))	244
Electrical power output (kW(e))	10 net
Net efficiency (%)	4.1
Operating life at full power (yr)	10
Reactor	
Core outside diameter (in.)	20.5
Fuel-zone thickness (in.)	0.59
Moderator-zone thickness (in.)	1.00
Temperatures (°F)	
Average core-hydride	1500
Average reservoir	1650
Average fuel	1424
Maximum fuel	1553
U-235 loading (kg)	11.6
U content of U-Zr alloy (wt %)	20
U-Zr loading, core (kg)	61.8
Zr loading, moderator and reservoir (kg)	200
Density of hydride materials (% of theoretical)	80
Cu reflector thickness (in.)	6.0 minimum
Thermoelectric Generator	
Element configuration	Encapsulated
P-type material	GeTe-$AgSbTe_2$
N-type material	3M-2N
Element diameters (in.)	
P	1.06
N	1.28

Table XII (cont'd)

Element thickness (in.)	0.100
Junction temperatures, End-of-Life (° F)	
Hot	840
Cold	292
Generator efficiency, End-of-Life (%)	5.5
Couple arrays (No.)	22
Couples per array (No.)	28
Total couples (No.)	616
Parallel banks (No.)	2
Series couples per bank (No.)	308
Full load, dc (volts)	30
Maximum current (amperes)	444
Blower	
Power output (bhp)	1.5
Air flow (lb/hr)	65,000
Nominal air temperature (°F)	
Inlet	70
Outlet	120
Fan and motor efficiency (%)	65
Net auxiliary power (kW)	2.0
Power Conditioner	
Output power (kW(e))	10
Output, dc (volts)	28
Conversion efficiency (%)	90
Output power stability	Meets MIL-STD-704A
Weight and Cost Estimate	
Active power plant weight (lb)	9170
Total cost based on production rate of 200 units/yr ($) (Does not include shielding, ducting and installation costs.)	162,700

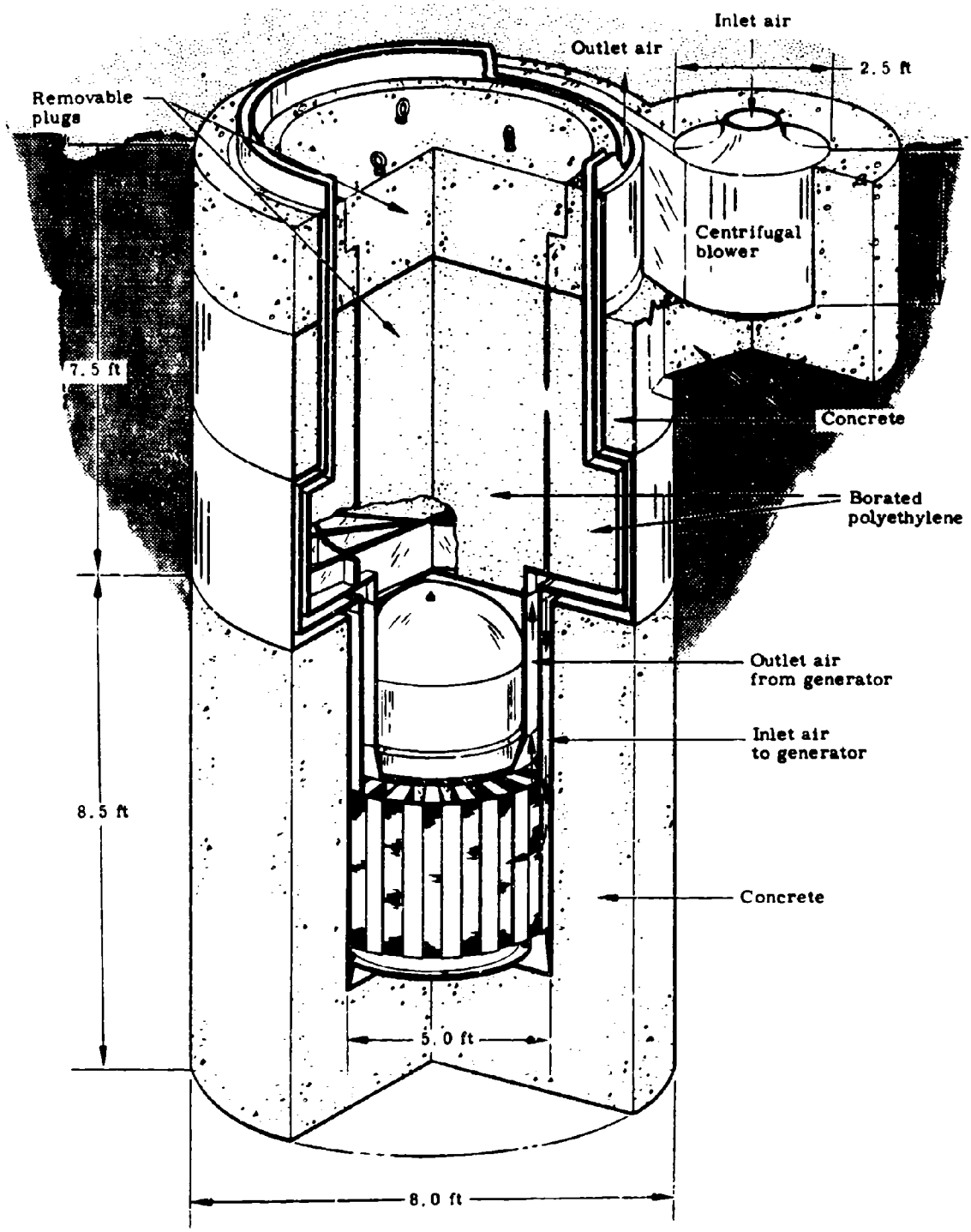

Figure 12. Installation of Direct-Conduction Reactor System

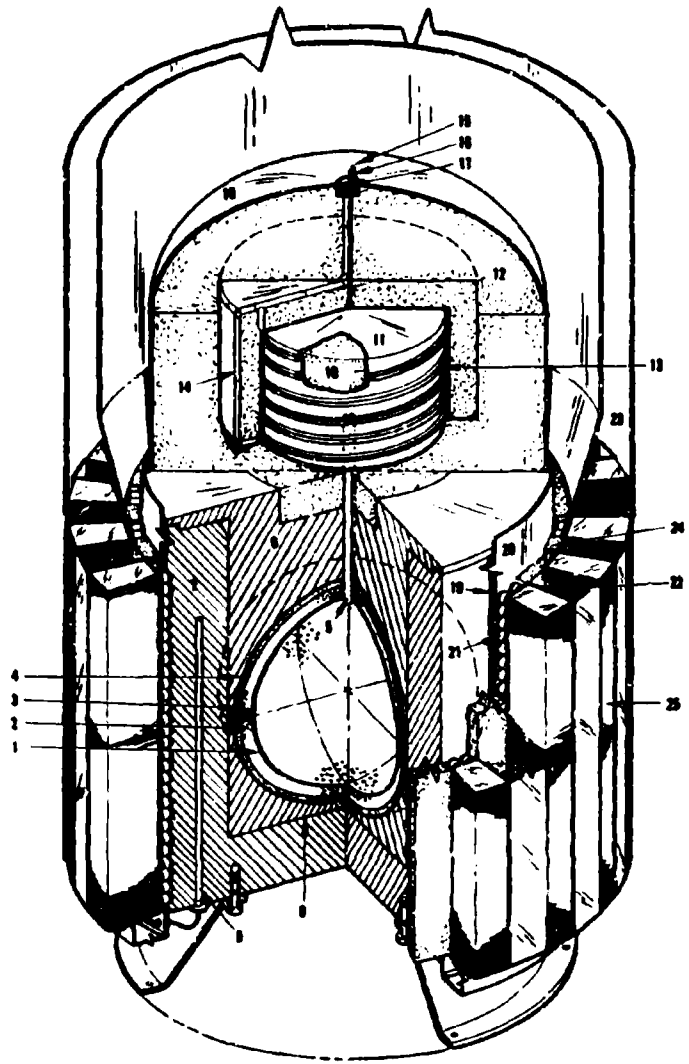

1. Inner core shell, perforated
2. Moderator
3. Fuel
4. Outer core shell
5. Hydrogen balance pipe
6. Inner copper
7. Outer copper
8. Inner braze surface
9. Electrical heaters
10. Porous zirconium hydride reservoir
11. Reservoir container
12. Thermal insulation
13. Electrical heaters
14. Electrical lead passage
15. Evacuation pinch-off
16. Hydrogen charge line and pinch-off
17. Heater terminals
18. Housing shell
19. Braze surface
20. Thermoelectric mounting shell
21. HPD thermoelectric elements
22. Cooling air ducts
23. Inlet air duct
24. Insulation
25. Cooling fins

Figure 13. Direct Conduction H-Rho Reactor-Thermoelectric Generator

The battery bank (for reservoir heating), power conditioner, and instrumentation are designed for 10-year performance. However, these are accessible because they are located outside the generator shielding.

This reactor power plant is unique in that it operates totally unattended and requires no scheduled maintenance. Moreover, it can handle steady-state and transient loads without human surveillance.

2. Analysis

a. Nuclear Analysis

(1) Method

A primary goal in the reactor design effort is to provide short heat transport paths. Thus, nuclear studies were directed toward investigating means of minimizing fuel region thickness. To this end, it was learned that a spherical shell fuel region surrounding a spherical shell moderation region yields high neutron economy while maintaining adequate hydrogen worth. The optimum moderator thickness for the core sizes of interest is about one inch.

Additional studies of reflector configuration yielded a minimum copper thickness of six inches from neutron economy and shielding considerations. Thus, with a lower limit of copper outer surface area provided by the power-density capabilities of thermoelectric elements, a lower limit to the core-plus-reflector diameter was set. From this point, reactivity and thermal constraints dictated the feasible region of core diameter and fuel region thickness.

(2) Results

(a) Initial reactivity: Preliminary nuclear and thermal analyses indicated that a fuel region of about 3/4-inch thickness and 24-inch diameter would be satisfactory. Hence, core dimensions and fuel density were studied parametrically about these values.

The relationship between core diameter and fuel thickness yielding sufficient reactivity for 10 years of operation at 200 kilowatts(t) is shown in

figure 14 for 10 and 20 weight percent U alloy fuel compositions. It is seen that about 0.3-inch greater thickness is required for the lower uranium density matrix. However, despite the larger fuel volume, a 30 percent lower fuel loading is exhibited by the 10 weight percent core (figure 15). Thus, selection of an optimum core configuration must consider evaluation of the effects of core dimensions and fuel loading upon the overall system cost. At present, it appears that the larger diameter, lower uranium density core (required to compensate for increased fuel thickness and fuel temperature constraints) imposes larger penalties upon the total system performance than the fuel savings. Thus, a 20 weight percent fuel matrix was selected.

Increasing the uranium density above 20 weight percent incurs large incremental fuel-loading penalties and decreased hydrogen worth. The reactor becomes less thermal and the control capability is reduced. These facts, coupled with uncertainties in fuel-matrix integrity (because of lack of experimental data) prevent use of higher uranium density at present.

(b) Depletion and control: Because of the high reliability and long life of thermoelectric elements, together with the high fuel loading requirement for criticality in the hollow spherical core, a 10-year design life was selected for the direct conduction power plant. Fuel burnup and fission-product accumulation for 10-year operation requires about one kilogram more U-235 or only 10 percent more fuel than for five-year operation. This is a small price to pay for doubled plant life.

The reactivity inventory for the conduction core is summarized in table XIII. It is seen that with an average hydrogen worth of 0.20 $\Delta\rho/\Delta X$, adequate control exists for 10 years of operation. As described in Section II, burnable poison could be used to reduce hydrogen concentration variation or increase the control margin. By allowing a 50° F drop in core temperature, one adjustment of the reservoir heaters is required, at the five-year mid-point. Further, by the use of a small amount of burnable poison (1.5 percent $\Delta\rho$ worth), the adjustment can be eliminated for up to 10 years of operation. For a detailed discussion of the reservoir-core temperature interaction, reference 3 should be consulted.

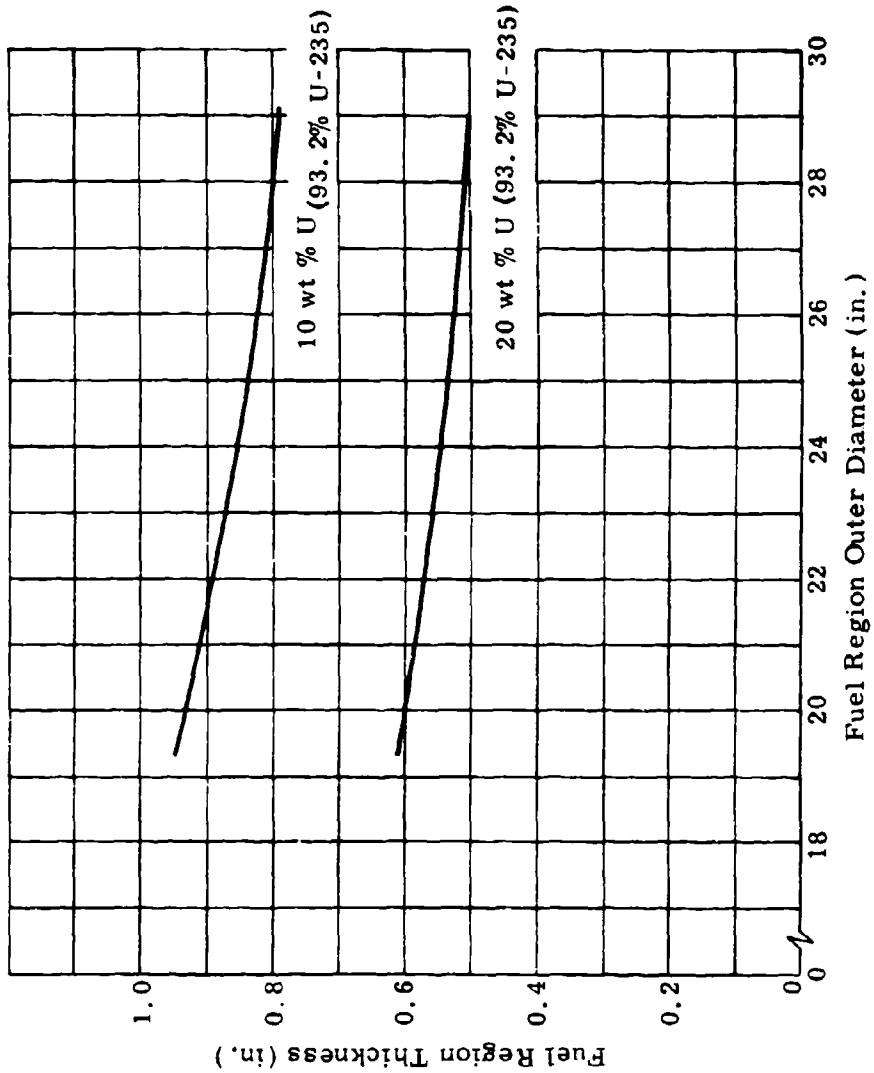

Figure 14. Relationship Between Fuel Region Thickness and Outer Diameter for 10-Year Operation at 200 Kilowatts(t)

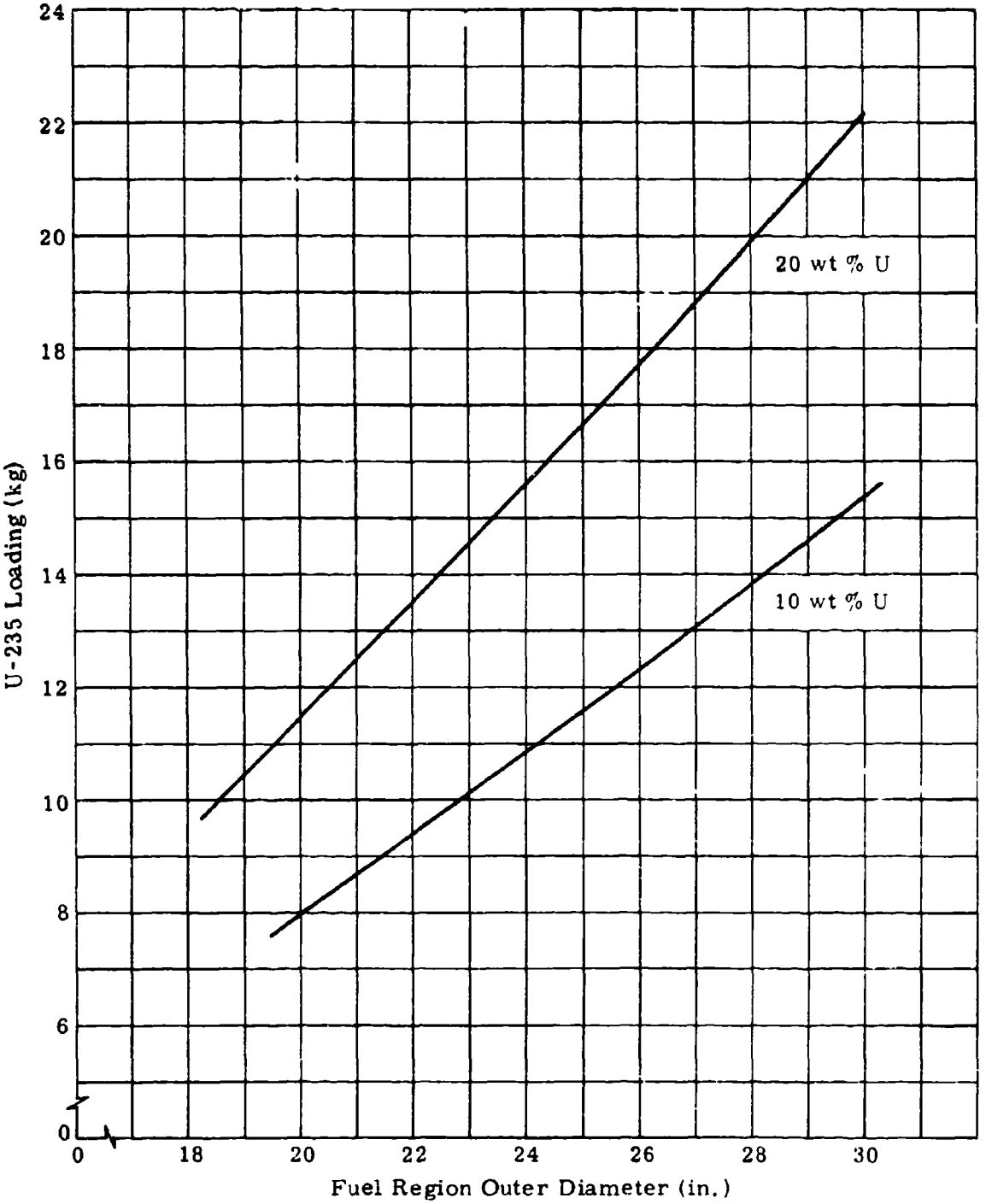

Figure 15. Variation of Fuel Loading with Fuel Region Outer Diameter

Table XIII

REACTIVITY INVENTORY FOR CONDUCTION-COOLED CORE

Quantity	% Δρ
Shutdown to cold critical	1.5
Cold critical to hot full power	2.0
Equilibrium fission products	1.0
Fuel burnup	3.0
Total	7.5

Average hydrogen worth = 0.20 $\Delta\rho/\Delta X$

Excess control margin for X from 1.45 to 1.85 = 8.0 - 7.5 = 0.5%

(c) Power peaking: Because of the spherical symmetry and small shell thickness, power peaking effects are insignificant in the reactor. Calculations have revealed that uniform power generation throughout the fuel matrix yields temperature profiles that are virtually identical to those obtained by considering the small amount of peaking at the core surfaces and depression near the center. Thus, uniform power generation was used in all parametric studies of thermal performance.

(d) Shielding: The operational shielding requirements for the direct-conduction reactor are similar to those for the Stirling plant because of the similarity of thermal power levels. Thus, a surrounding shield of 18 inches of ordinary concrete is required to prevent significant ground activation.

Personnel shielding will be provided by borated polyetheylene and concrete layer regions above the power plant. Dose rates will be limited to approximately 20 mr/hr at the shielding surface by using five feet of polyethylene

followed by two feet of concrete. The cooling air passages are stepped to prevent excessive radiation streaming. Air activation is rendered negligible by lining the air passages near the core with boral.

The power plant is designed for unattended operation so that no direct accessibility to the thermoelectric converter is provided during operation or after reasonable shutdown periods. Maintenance will consist solely of replacement. Repair, if desired, can be performed at specially designed factory facilities.

b. Thermal Analysis

(1) Method

The removal of heat from a nuclear heat source can be accomplished in a variety of ways. For high power applications it is usually done by circulating a coolant through the heat source. Coolant passages are formed either by holes in the fuel material or by spaces between fuel particles or elements. Examples of this approach include all large power reactors. The introduction of coolant into the heat source has certain disadvantages. The plumbing is usually complex and expensive. Coolant compatibility with materials of construction and with the radiation environment becomes critical. The cooling system itself adds significantly to the complexity of the power plant: valves, pumps, seals, coolant conditioning devices, etc. If the heat source is a nuclear reactor, the effects of the coolant on neutron economy and power peaking can be detrimental to the plant economics. For very low power applications, the disadvantages of a coolant system outweigh its benefits, and heat should be removed by conduction. Examples of this approach include most of the SNAP isotopic power devices.

In the design of unattended power devices it is prudent to explore the feasible power range of conduction-cooled devices as they promise simple, more reliable operation. In general, the power density of a device cooled at its surface by direct-conduction is much lower than that of an internally cooled one for a given temperature limitation. As the power requirements increase, the size of the

heat source must increase. The power range of applicability is set by operational and economic factors. A coolant is introduced only when the advantages of simplicity and reliability are offset by high costs.

A nuclear reactor heat source has two unique features which influence its thermal design.

(a) There is some minimum size and fuel content below which it cannot function.

(b) It can operate at any power density consistent with the limiting temperature and heat removal system.

From the first, it is concluded that core complexity, size and cost are bounded from below, independent of power level. From the second it can be seen that for a desired total power the volume of fuel is not fixed, but may be selected to satisfy the criticality and thermal constraints without regard to power density. Additional limitations which stem from fuel burnup considerations play only a secondary role in setting the power density of low power devices.

Consider, as an illustration, a spherical core, with uniform power distribution. The power level is limited by the fuel temperature, T_f. Then for some given surface temperature, T_o, the following equations apply. For a solid sphere,

$$q = 8\pi k (T_f - T_o) r \tag{1}$$

and for a thin spherical shell

$$q = 8\pi k (T_f - T_o) r (r/t) \tag{2}$$

where

q = power
k = thermal conductivity
T_f = maximum allowable fuel temperature
T_o = surface temperature
r = radius of sphere
t = shell thickness

It can be seen from equations (1) and (2) that while the solid sphere size is fixed for a given power, the shell is not. Within a given radius, a shell can produce any power provided (r/t) is the proper value. For the spherical shell configuration, the thermal constraint is removed and the problem is reduced to selecting dimensions that satisfy the nuclear design. That is, for any radius, r, a fuel thickness, t, must be selected to meet the needed reactivity requirements. This critical configuration will have a certain power capability according to equation (2).

It is clear that the smaller the fuel thickness, the larger the power capability. The fuel composition should be selected to allow a minimum t if power is to be maximized.

(2) Results

(a) Core selection: The thermal requirement for the core under consideration is estimated from the desired net output of 10 kilowatts, the reservoir heater requirement of 200 watts, and the blower power of two kilowatts. At five percent electrical efficiency, 244 kilowatts(t) are required.

Figure 14 shows the relationship between fuel region thickness and core outside diameter that satisfies the reactivity requirements for 10-year operation at 200 kilowatts(t).

By using the dimension constraints from Fig. 14 in the thermal power calculations outlined above, a core capable of delivering 200 kilowatts(t) was defined. A similar procedure for other power levels was followed to yield the ranges of thermal capability presented in Fig. 16. It should be noted that constraints on copper thickness and surface temperature were included to meet other design requirements. The copper thickness, for example, was based on its effectiveness as:

1. A neutron reflector
2. A shutdown and operational shield
3. A heat conductor
4. A heat flux attenuator.

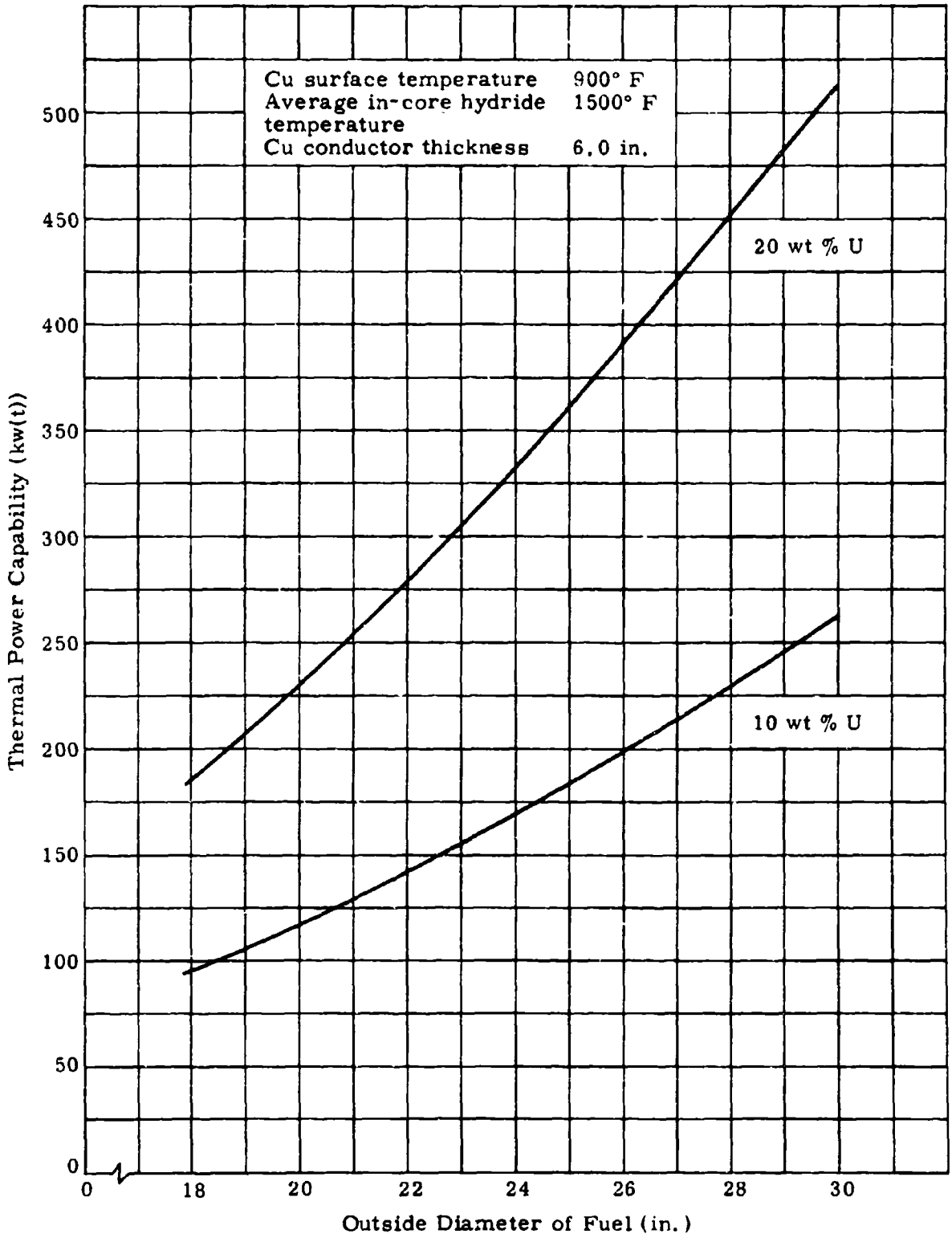

Figure 16. Effect of Core Size and Fuel Composition on Thermal Capability

The copper surface temperature was chosen to provide the needed hot junction temperature on the thermoelectric elements in the generator. The average hydride temperature was selected to satisfy H-Rho control requirements.

By selecting a 20 weight percent U-235 fuel matrix, a core with a 20.5-inch outside diameter can be used to produce 244 kilowatts(t). Using a 10 weight percent fuel would require a core 29.0 inches in diameter which would contain 25 percent more fuel. There still appears the possibility of selecting an even higher weight percent fuel form, producing a smaller core. Limiting factors here include ease of fabrication and nuclear design considerations as discussed previously.

(b) Temperature distribution: Figure 17 gives the temperature distribution through the midplane of the core and surrounding copper. There will be a longitudinal temperature gradient along the face of the copper block and a circumferential gradient about the core surface. However, these effects are minimized by the high conductivity of the copper.

It is evident from figure 17 that temperature gradient through the unfueled moderator region is negligible. The major gradients occur across the fueled segment and the fuel-clad copper interface. In the case shown the fuel thickness is 0.59 inch, and the outside radius is 10.30 inches. Thus, the thermal power extracted for the maximum fuel temperature shown is 10.30/0.59 or 17.5 times the power possible from a solid sphere of equal outer dimensions.

The copper conductor proves efficient in minimizing temperature peaks resulting from the asymmetric heat removal obtained by burying a spherical core in a cylindrical conductor and removing heat from the sides. The results of two-dimensional heat conduction calculations are shown in figure 18. Isotherms are expressed as relative to the temperature at the outer face of the copper conductor. Note that only a 35° F variation exists along the outer face where the thermoelectric modules will be attached.

The copper surface temperature was chosen to provide the needed hot junction temperature on the thermoelectric elements in the generator. The average hydride temperature was selected to satisfy H-Rho control requirements.

By selecting a 20 weight percent U-235 fuel matrix, a core with a 20.5-inch outside diameter can be used to produce 244 kilowatts(t). Using a 10 weight percent fuel would require a core 29.0 inches in diameter which would contain 25 percent more fuel. There still appears the possibility of selecting an even higher weight percent fuel form, producing a smaller core. Limiting factors here include ease of fabrication and nuclear design considerations as discussed previously.

(b) Temperature distribution: Figure 17 gives the temperature distribution through the midplane of the core and surrounding copper. There will be a longitudinal temperature gradient along the face of the copper block and a circumferential gradient about the core surface. However, these effects are minimized by the high conductivity of the copper.

It is evident from figure 17 that temperature gradient through the unfueled moderator region is negligible. The major gradients occur across the fueled segment and the fuel-clad copper interface. In the case shown the fuel thickness is 0.59 inch, and the outside radius is 10.30 inches. Thus, the thermal power extracted for the maximum fuel temperature shown is 10.30/9.59 or 17.5 times the power possible from a solid sphere of equal outer dimensions.

The copper conductor proves efficient in minimizing temperature peaks resulting from the asymmetric heat removal obtained by burying a spherical core in a cylindrical conductor and removing heat from the sides. The results of two-dimensional heat conduction calculations are shown in figure 18. Isotherms are expressed as relative to the temperature at the outer face of the copper conductor. Note that only a 35° F variation exists along the outer face where the thermoelectric modules will be attached.

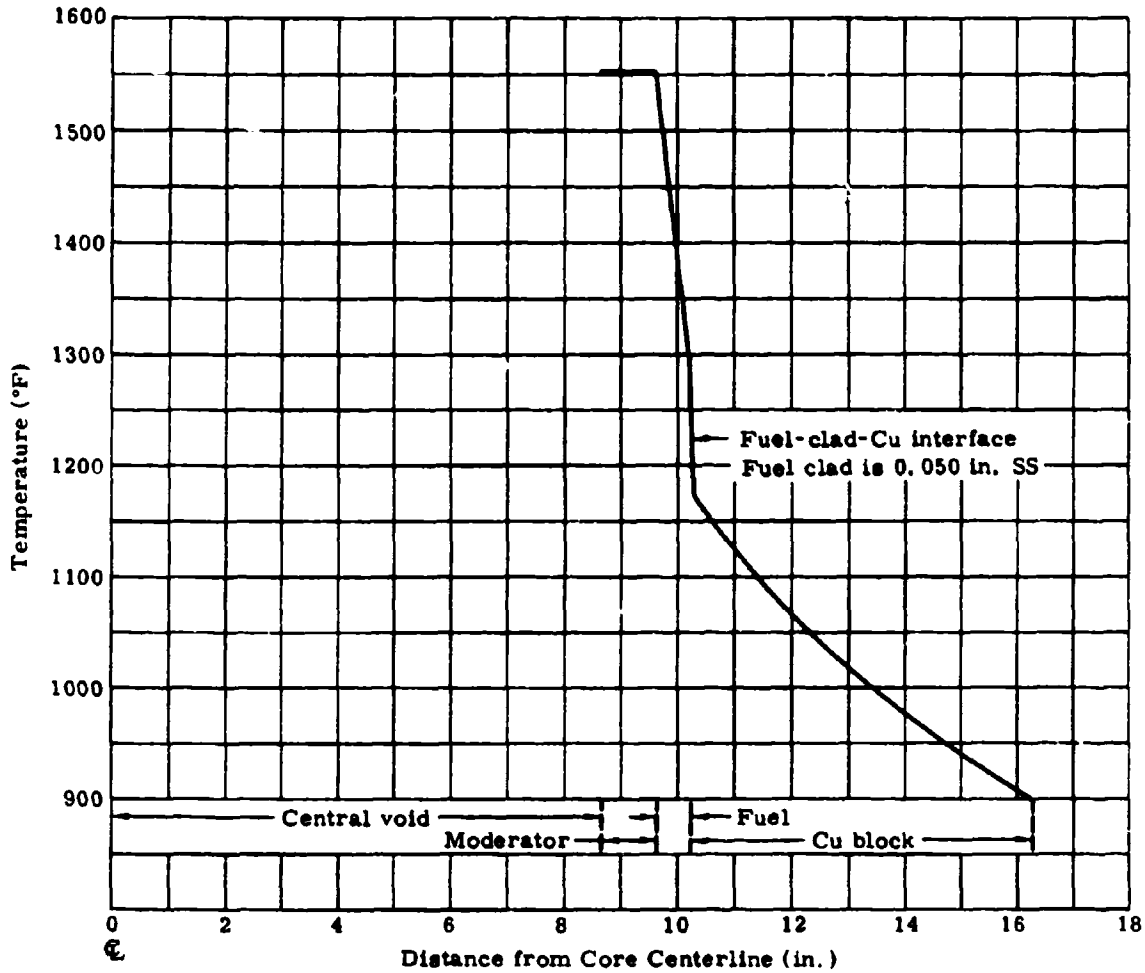

Figure 17. Temperature Distribution Through Mid-Plane at 244 Kilowatts(t)

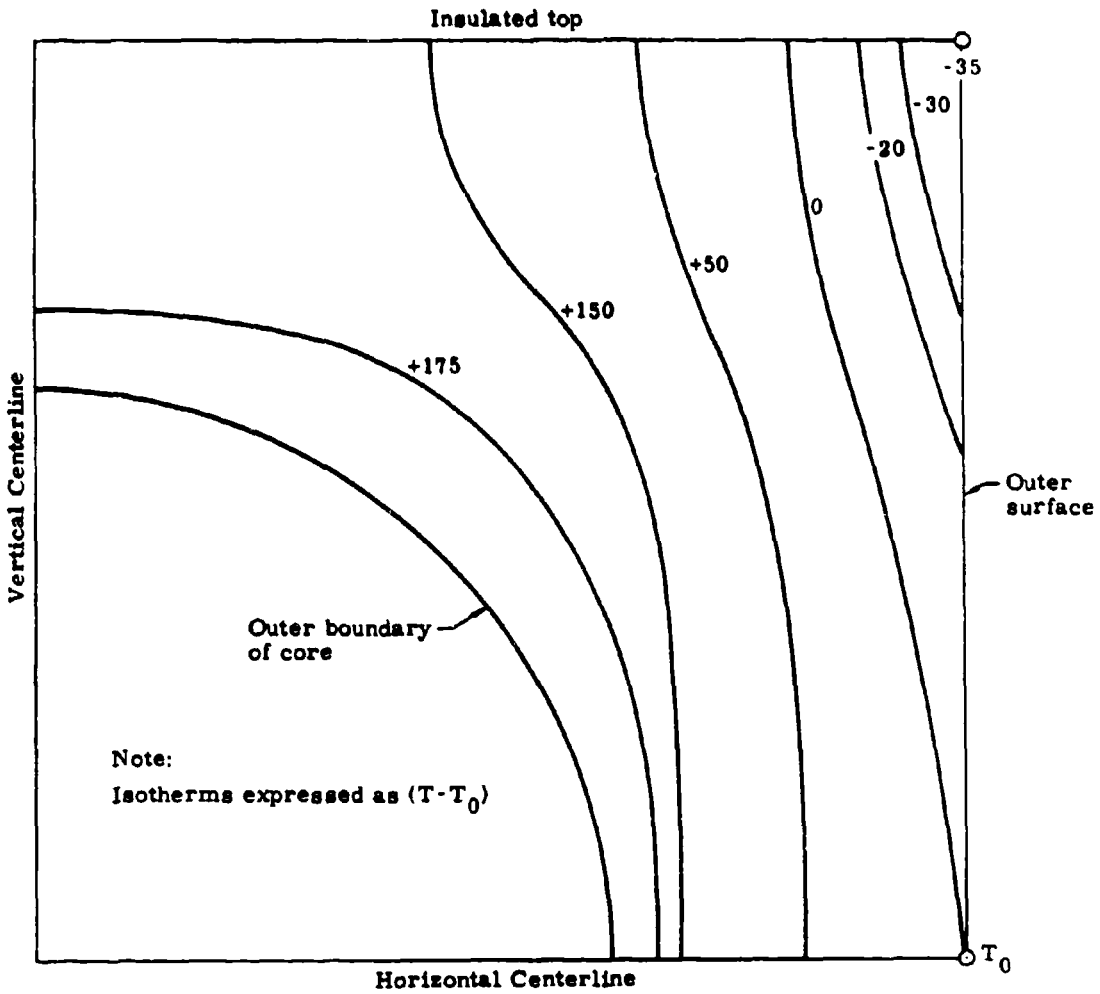

Figure 18. Temperature Distribution in Copper Conductor

c. Dynamics Analysis

(1) Method

The principal effect of a load change in this thermoelectric system is a change in the magnitudes of the Peltier sink and source terms at the hot and cold junctions, respectively, of the thermoelectric material. The dynamics model used the heat capacities of the core, the massive copper block surrounding the core and the thermoelectric materials. The heat transfer analysis was a quasi-steady-state model relating the heat flux between regions to their average temperatures. Included were the electrical current-dependent sources and sinks (Peltier, Thompson and resistance) in the thermoelectric region. A constant coolant temperature was assumed, and the temperature rise to the thermoelectric region cold junction was assumed proportional to the exit heat flux. The H-Rho control system, as in the Stirling system analysis, assumed steady-state hydrogen concentration as a function of fuel temperature, neglecting any transport or diffusion delays. The core power level-reactivity feedback loop utilized a single delayed group neutron kinetics model. The integration of these coupled differential equations was done by digital computer using DSL.

(2) Results

The combination of the extremely large heat capacity of the core and copper regions and the phenomenon that large percentage changes in electrical load result in small percentage changes in the thermal load yield a system that, thermally, is relatively insensitive to load changes. That is, the electrical demand is satisfied immediately and very small, slow changes of core power and temperature distribution occur. In figure 19 the core power response in the first 2500 seconds of 8.4 to 12 and 12 to 8.4 kilowatt(e) step changes in load are shown. The 30 percent (of full electrical) power) load change corresponds to only a 2.8 percent change in core thermal output. In addition, the maximum change in average fuel temperature is very small ($\sim 0.05^\circ$ F), with the corresponding maximum core reactivity

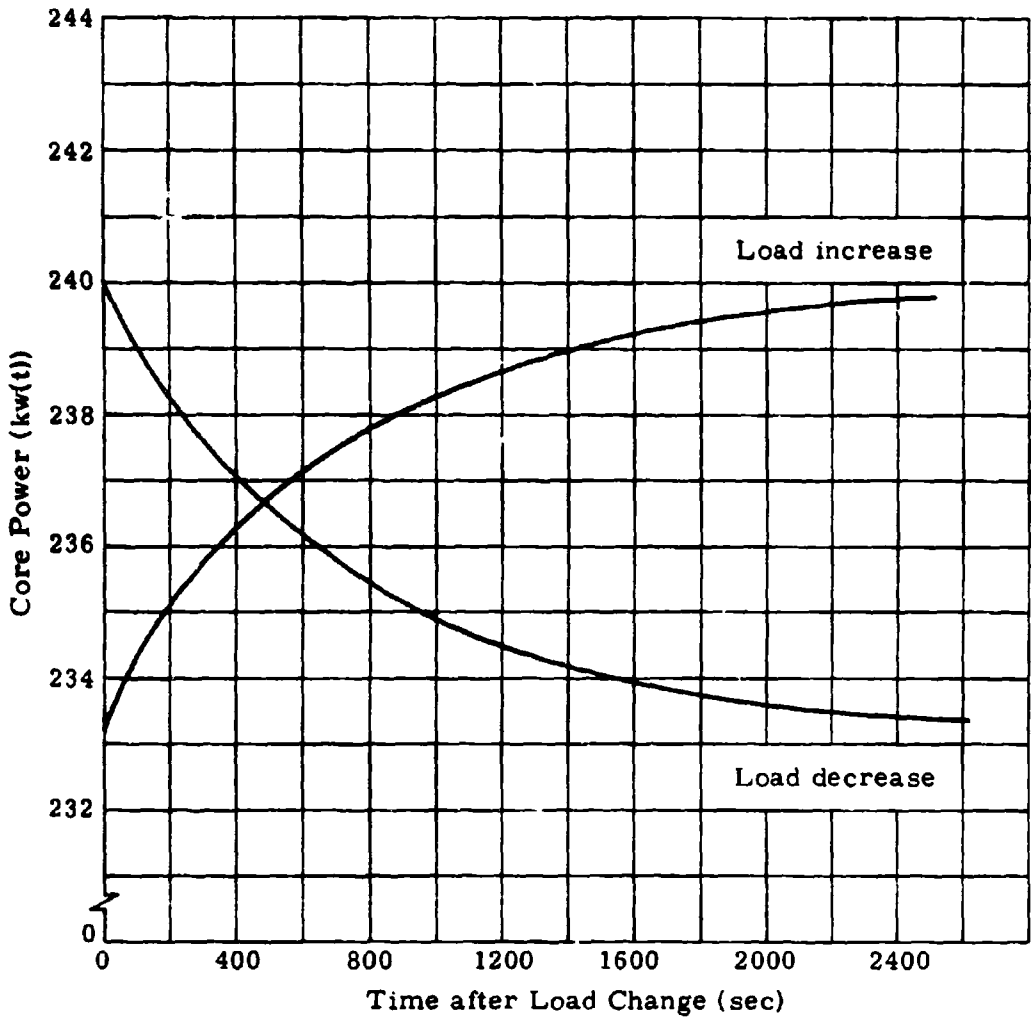

Figure 19. Thermal Power Response of Thermoelectric System for Step Load Changes from 70 to 100% and 100 to 70% Power

being only 6×10^{-6} $\Delta\rho$. These transients are undoubtedly overdamped, and the asymptotic approach to the final steady-state values is apparent.

d. Systems Design--Mechanical and Electrical

(1) Method

The functional simplicity of direct conduction-cooling and mechanically passive thermoelectric conversion reduces the principal task of mechanical design to one of providing good heat transport paths to avoid undesirable temperature gradients. In addition, the thermoelectric generator and the conditioning of its power output to the desired form, are discussed in detail because of their importance to the system design. The following paragraphs contain a description of the mechanical configuration with brief comments on assembly procedures to highlight the significant features. To aid comprehension, the function and purposes of some components are also included. References to figures 12 and 13 are not made explicitly, but familiarity with these drawings is basic to the understanding of all design characteristics.

As a further descriptive aid, figure 20, a schematic of the power source, is presented. It includes the major system components. The reactor core, thermoelectric generator, heat removal subsystem, instrumentation and control package and the power conditioning subsystem interrelationships are depicted.

(2) Discussion

(a) Reactor: The reactor is comprised of a core, a hydrogen reservoir and a heat block assembly. It is H-Rho controlled and conduction cooled. The core is a concentric spherical shell arrangement of structure, moderator and fuel. It is contained in a high nickel alloy outer clad and bonded within the massive copper heat block. The porous uranium-zirconium hydride fuel is positioned directly against the outer clad and forms a shell 0.59 inch thick. Within this is a concentric shell of unfueled zirconium hydride which serves as a moderator. The two hydride shells are held in place by a thin inner spherical shell of high nickel alloy. This shell is perforated to allow the free flow of hydrogen. A relatively large void region exists at the center of the core.

Although little information is available on U-ZrH_x with more than 20 weight-percent U, mechanical property data[8] indicate that basic zirconium lattice structure exists below 40 weight percent U in Zr alloys. Thus, condition of phase transformation and fission product release in 20 weight percent U-ZrH_x

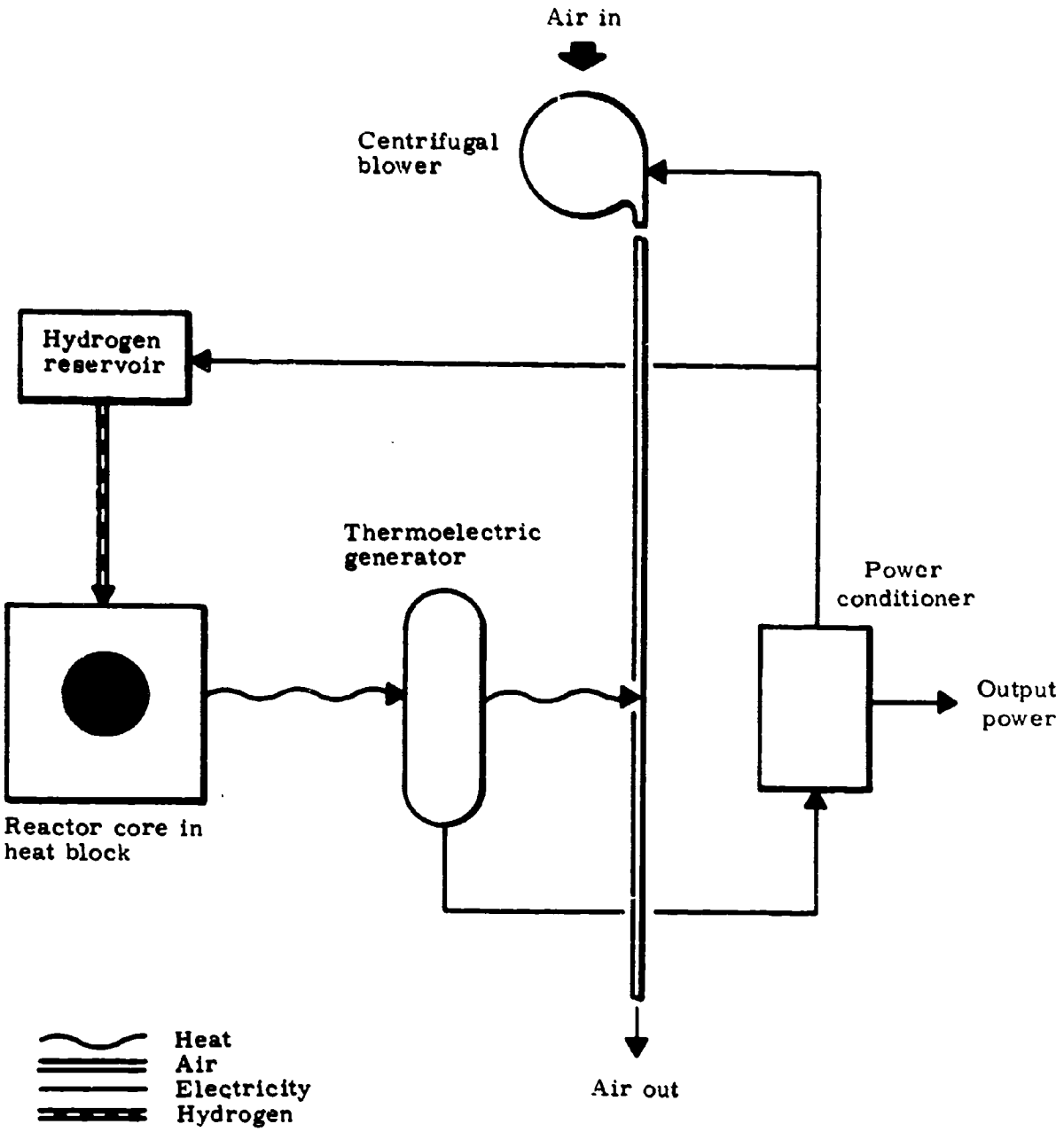

Figure. 20. Schematic of Condition-Cooled Reactor

is considered similar to that in 10 weight percent U-ZrH_x. In any event, the low burnup in this core indicates that gross fission product release into the hydrogen passages will not affect H-Rho control action significantly[5].

The zirconium hydrogen reservoir that provides the means to control the fission process acts as a source and sink of hydrogen. The porous zirconium hydride is arranged to provide easy passage of hydrogen gas through the material. A gas passage links the core and reservoir. To ensure fail-safe functioning of the H-Rho control scheme, the reservoir region must be kept at a temperature higher than that of the hydride material in the core. This is accomplished by using a small portion of the plant power output (200 watts) to operate heater elements wrapped about the outer surface of the reservoir container. The entire reservoir region is insulated to sustain this low power requirement. Two high-current, high cross-sectional area heaters that operate at 1700° F are used. A single heater can maintain the reservoir temperature but redundancy is provided despite design features indicating essentially infinite life expectancy of the heater.

The heat block assembly consists of two mated copper pieces that form an enclosure of the spherical core. The primary purpose of the heat block is to transfer heat from the core to the thermoelectric generator. Interfaces are metallurgically bonded to reduce temperature drops in transition areas. Boron deoxidized copper is the heat block material since this alloy maintains high conductivity throughout fabrication procedures and has improved resistance to embrittlement.

Primary fission product retention is provided by the outer core clad, the gas passage tube between the core and reservoir and the reservoir container. Because of the high operating temperatures of these surfaces, only token hydrogen containment is provided here. The secondary fission product seal, formed by the heat block itself and an outer container sealed about the reservoir insulation, provides the major barrier to hydrogen loss from the system.

During startup, the core temperature must be elevated to permit rapid movement of hydrogen within the hydride materials. For this purpose, 12 start-up heaters are embedded in the heat block. They have a total capacity of 250 kilowatts. During checkout of the power source at the manufacturing facility, these are operated at their rated power, thereby allowing a full

power check of the electrical system and generator. At the site, about 50 kilowatts will be required to achieve criticality. This power will be provided by an auxiliary power source.

(b) **Thermoelectric generator:** The generator design is based on the use of encapsulated high-power density thermoelectric elements. Individual jackets control the operating environment of the element and provide a normal force to maintain physical integrity of the assembly. The elements are assembled into 28 arrays or modules. Elements of each module are series-connected. The modules, in turn, are connected in two parallel banks to provide the needed voltage. A value in excess of the required 28 volts dc is generated to allow for losses incurred in power conditioning.

Figure 21 shows the element reference design. The active wafer materials are germanium telluride (TAGS-85 formulation) for p-type elements and lead telluride (3M-2N formulation) for n-type elements. The wafer thickness for both types is 0.100 inch. The n-element is bonded to an iron diffusion barrier with nickel; the p-element is bonded to a tantalum diffusion barrier with silver and tin. The diffusion barriers are bonded to copper heat distribution plates that, in turn, are held by rigid composite shoes of high nickel alloy and copper. The jacket of high nickel alloy has a flange at the cold end which is sprung by a force of 200 pounds during assembly. The flange bears on a loading plate that is electrically insulated by fused glass so that the jacket does not electrically short the element. The jacket closure weld is made under vacuum.

The major objective and problem in thermoelectric design is to make devices that do not degrade in performance with time. The processes of degradation of tellurium alloy thermoelectrics can be both chemical and mechanical. The solution to the chemical problem appears to be to avoid contacting the thermoelectric material with materials which react with it. The use of nonreactive diffusion barriers and vacuum encapsulation has been successful in this regard. The solution to the mechanical problem appears to be to use enough clamping force. The amount of force required, of course, depends on the magnitude of the forces tending to disrupt the quality of contact to the thermoelectric material.

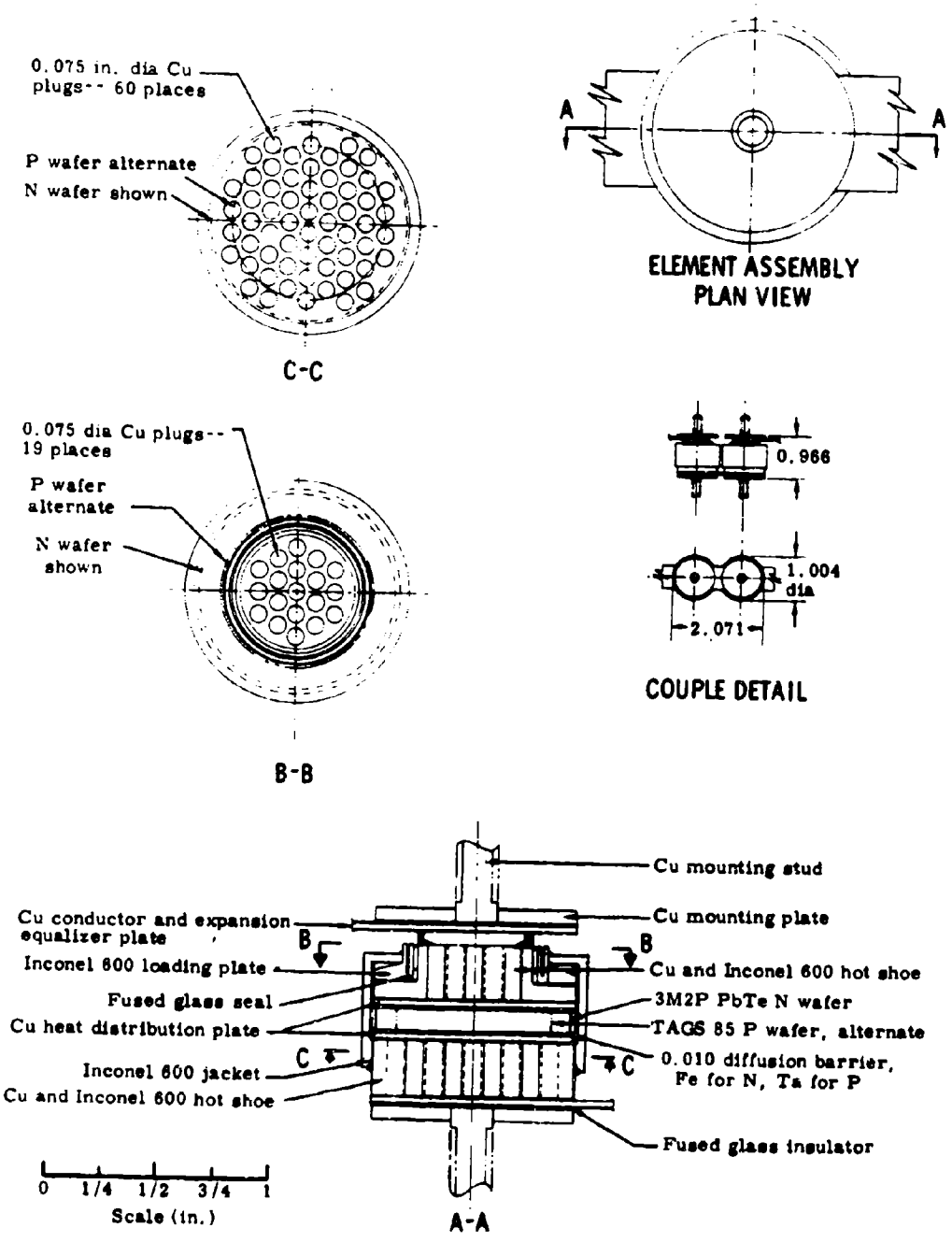

Figure 21. Jacketed Thermoelectric Element for Generator of Nuclear Power System

The practical difficulty in establishing the drift rate of good thermoelectric devices is that a relatively long test time is required before the drift clearly rises above the measurement errors. Using experimental data autocorrelated to remove a two-percent random measurement error requires 6000 hours to establish a drift rate of one percent per year. If the degradation processes are mechanical, the testing can be accelerated by thermal cycling. Although a correlation between steady operation and thermal cycling has not been established, some state-of-the-art operational devices, which operate well for five years, will not survive thermal cycling at all.

High-power density thermoelectric elements of essentially the same configuration as figure 21 have been operated for about 1000 hours and subjected to severe thermal cycling. Figures 22 and 23 show the measured power output and efficiency of the latest p- and n-elements. The p-element did not happen to be jacketed; it was hydraulically clamped at 400 pounds. The n-element jacket had a defective seal; it was operated in an argon-filled tester. Both elements appear to have acceptably small degradation rates.

The module cold-ends are extensively finned to allow air cooling. Air flows down an outer annulus radially through the fins and up through the ducts between adjacent modules.

(c) Heat removal subsystem: A centrifugal blower is used to circulate air through the cooling ducts. Cold air enters the blower and is forced down through channels in the shield assembly and into the region of the finned thermoelectric modules. The exhaust is vented directly to the atmosphere. The air experiences a 50° F temperature rise. A limited amount of heat (about 25 percent) can be removed by natural circulation. This provides for emergency cooling in the event of blower failure.

(d) Instrumentation and control: The H-Rho control system obviates the need for complex nuclear instrumentation. It is sufficient to monitor the thermal state of the device to determine its performance. During startup, reactivity insertions are strictly controlled by power input, system heat capacity and heat loss. The rates can be limited through design to ensure

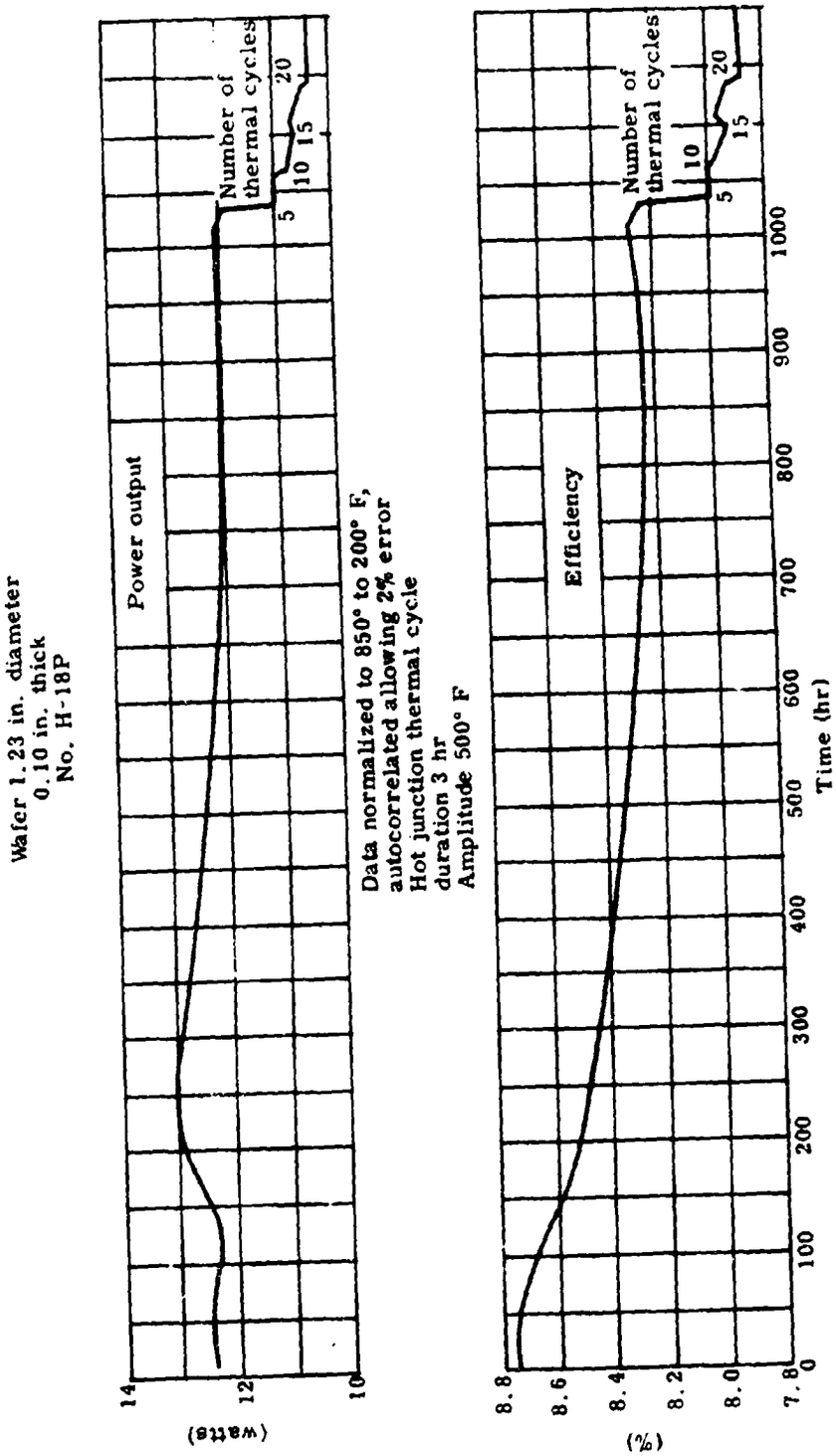

Figure 22. Performance of P Element Clamped by 400 psi

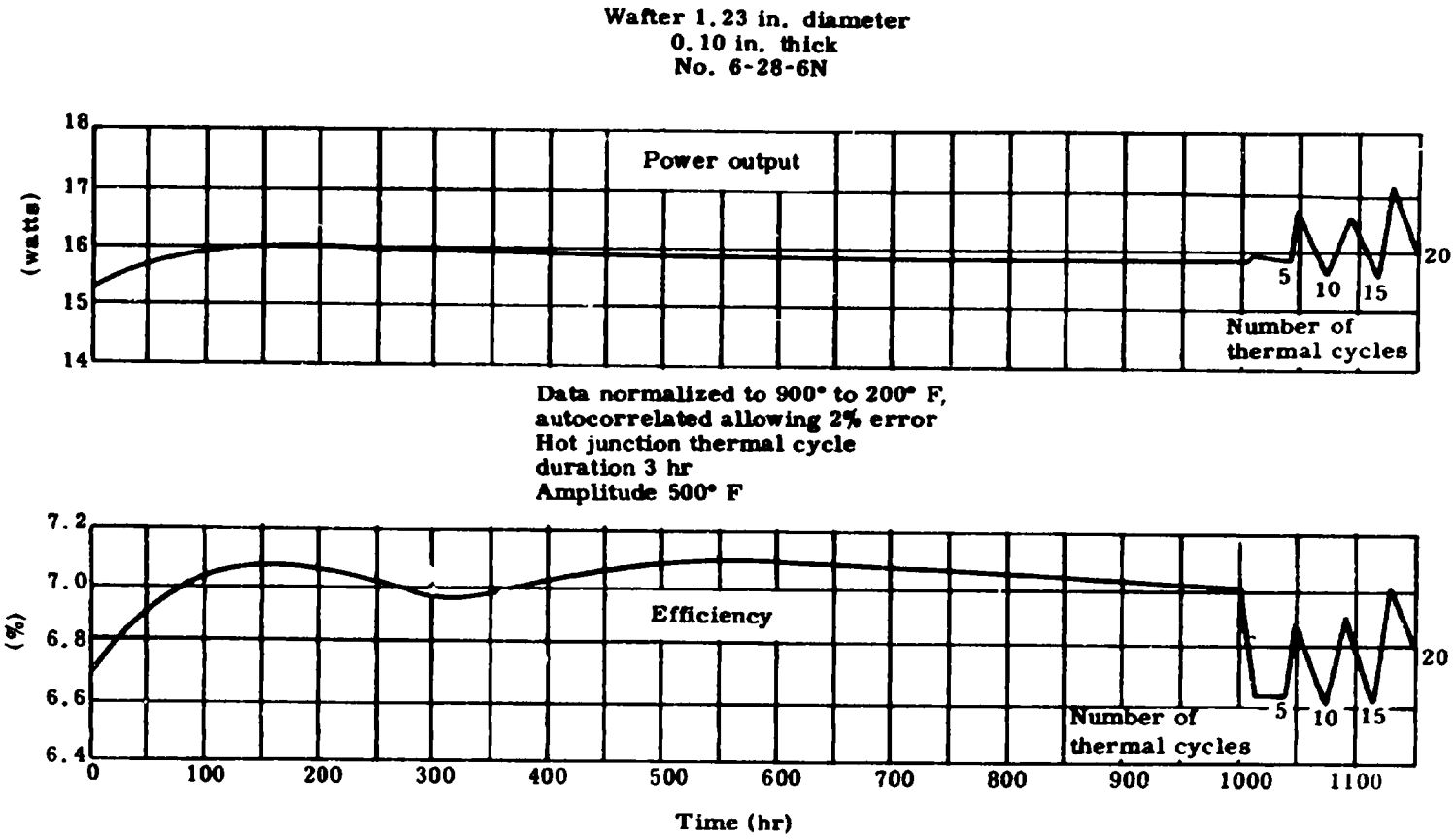

Figure 23. Performance of Jacketed N Element

safe startup. Instrumentation will consist of temperature and electrical output sensors with remote displays on the control console.

External control is limited to startup, shutdown and infrequent regulation of the reservoir heater power. These actions may be performed through electrical switching at the control console.

(e) Power regulation and conditioning: Because of the simple resistive nature of the source impedance of the thermoelectric generator, its output voltage is inversely proportional to the electrical power drawn from it. The generator terminal voltage varies from 60 volts when the load power requirement is zero to 30 volts at the full load of 10 kilowatts. The latter is approximately the maximum output power condition. Some feedback through the H-Rho reactor control system tends to modify the simple transfer characteristics of the generator, but the effect is small.

To provide essentially constant voltage output from the power plant, independent of load power requirement, a solid state voltage regulator is used between the generator terminals and the load. The regulation is provided by duty-cycle modulation. This type of regulation is nondissipative in the sense that, except for the power loss from regulator inefficiency, no power is dissipated within the regulator. The regulator periodically switches the generator on and off, varying the ratio of on-to-off time, such that the average value of the regulator output is 28 volts. The averaging process is performed by a passive filter of capacitors and chokes.

A functional diagram of the regulator is shown in figure 54. A transistorized chopping shunt short-circuits the generator at intervals of 8.3 milliseconds, the effective short-circuit time being approximately 0.3 millisecond. The average current handled by the shunt is 27 amperes.

After being chopped, the generator output is fed to a duty-cycle modulator that uses silicon-controlled rectifiers. The rectifiers cease to conduct each time the generator is shorted. A signal from the error amplifier returns the rectifiers to a conducting state after an appropriate delay. The silicon-controlled rectifiers handle the full load current of 350 amperes.

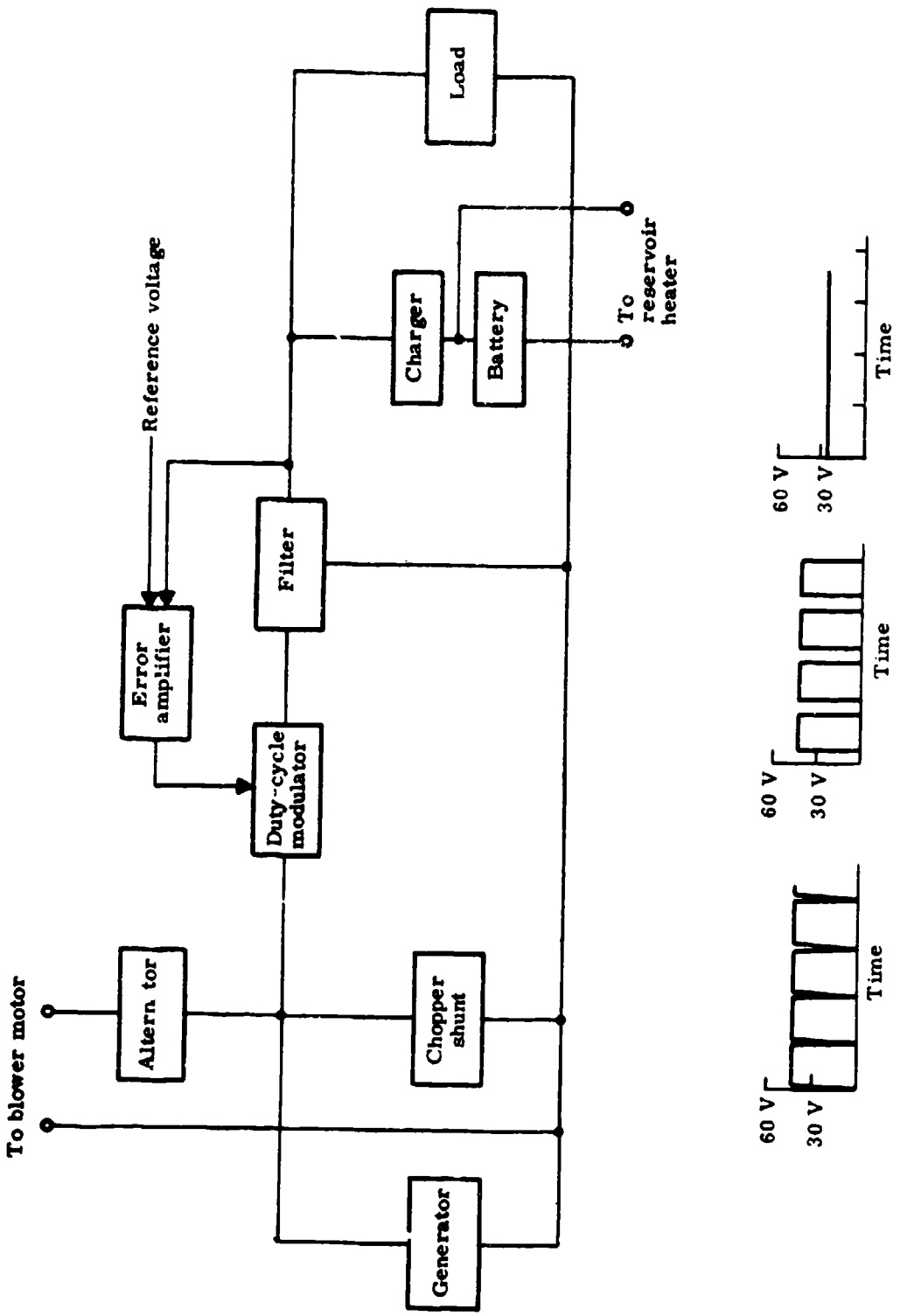

Figure 24. Power Conditioner

The error amplifier compares the voltage of filtered output with the reference voltage, determined by a small mercury battery, establishing the delay period.

Ahead of the duty-cycle modulator, two kilowatts are drawn to operate the blower. Chopped output is sent through a solid-state alternator that reverses the polarity of every other pulse. The consequent alternating square wave is fed to the 60-Hz induction motor that drives the blower.

In parallel with the load is a battery and charger. This battery supplies 220 watts to the reservoir heater and the plant instrumentation.

All power conditioning equipment is located outside the power plant. Although the life expectancy of such equipment can exceed the plant life, provision is made for replacement of defective units.

The power conditioner is a conventional design device. Full load efficiency is 90 percent. Its capability to regulate under both steady-state and transient load conditions will easily exceed accepted military specifications for direct current power sources (MIL-STD-704A).

e. Weight and Cost Estimate

(1) Method

Detailed weight and cost estimates were prepared only for the active generator components. Relatively inexpensive shielding, fixed ducting, and structural materials are transportable in bulk or are usually available at proposed sites for other purposes, hence only approximate volumes and weights are given. As noted, plant costs are strongly dependent upon rate and total quantity of production. The following values are based on a rate of 200 units per year. Reducing the production to 100 units per year will cause a cost increase of approximately 25 percent.

(2) Results

(a) Weight estimate: The weights of active generator components are presented in table XIV. It is apparent that the copper block comprises most of the plant weight. Therefore, final design modifications to the core, generator and cooling system will not affect total plant weight significantly.

Table XIV

WEIGHT ESTIMATE OF GENERATOR COMPONENTS

	Weight (lb)
Reactor core	395
Reservoir	235
Cu block	7280
Reservoir insulation and container	180
Thermoelectric generator mounting cylinder	250
Thermoelectric couples	250
Cooling fins and ducting	420
Electrical heaters	20
Centrifugal blower and motor	140
Total	9170

For shielding and structural purposes, approximately 16 cubic yards of concrete and 276 cubic feet of borated polyethylene are required. Access to the generator involves removing the shield plug, which consists of 5640 pounds of concrete and 5600 pounds of polyethylene.

(b) Cost estimate: A pricing effort and engineering evaluation of the 12-kilowatt(e) (gross) direct-conduction nuclear plant was conducted. The results, given in table XV, are based on a rate of 200 units per year and do not include shielding, ducting, and installation costs.

Since the production facility does not exist, labor, overhead and profit rates must be assumed. The following values, while hypothetical, are believed to be realistic and have been used in determining the selling prices in table XV.

	($/hr)
Manufacturing labor	8.50
Engineering liaison labor	14.50

Table XV

PRODUCTION PLANT COST ESTIMATES

	Cost ($)
Labor	84,600
Materials and subcontract	78,100
Total	162,700

This estimate includes materials and fabrication costs of the reactor core because the core is an integral part of the structure and cannot logically be priced separately. Additional expenditures usually included in an overall fuel-cycle cost, such as reprocessing, amount to about 2.0 mills/kW-hr, excluding burn-up and use charge. Because it has not been the custom in the past (e.g., PM-1, PM-3A) for the government to charge itself for fuel use, these charges are not included in the fuel cycle cost estimate. Tables XVI through XX list the fuel cycle parameters used in obtaining the fuel cycle cost. Table XXI itemizes the various costs in dollars per kilogram of initial uranium content. The design point selected here uses 12.4 kilograms of uranium and the total fuel cost is $17,707.

Table XVI

FUEL CYCLE PARAMETERS, SET BY DESIGN

Charged (% U-235)	93
Discharged (% U-235)	92
Thermal power level (kW(t))	244
Net power (kW(e))	10
Initial fuel loading (kg)	11.5 U-235
Total fuel discharged (kg)	10.6 U-235
Final plutonium inventory	Negligible

Table XVII

FUEL CYCLE PARAMETERS, TYPICAL VALUES SET BY INDUSTRY

Plant factor (%)	100
Shipping time--AEC to fabricator (days)	20
Conversion plant throughput (kg/mo)	4000
Irrecoverable losses (%)	
Conversion	1
Fabrication	1
Recycle losses (%)	10
Fabrication time (days)	90

Table XVIII

FUEL CYCLE PARAMETERS, TYPICAL VALUES SET BY AEC

Minimum time before reprocessing (days)	120
Irrecoverable losses (%)	
Chemical separation	1
Conversion	0.3
Rates (kg/day)	
Chemical separation plant processing	44
Reconversion	150

Table XIX

FUEL CYCLE PARAMETERS, ASSUMED INDUSTRIAL CHARGES

	($/kg U)
Conversion charges*	283
Shipping charge AEC to fuel supplier	1.50

*Extrapolated from data given in TID-7025 (volume 4)

Table XX

FUEL CYCLE PARAMETERS, ASSUMED AEC CHARGES

Prices ($/kg U)	
Uranium before use	10,385
Uranium after use	10,267
Conversion charges to UF_6	32.60
Shipping charge reprocessor to AEC	1.00
Separations plant daily charge ($)*	21,000

*Extrapolation at rate of $500/yr from $17,000 given in reference 7.

Table XXI

FUEL CYCLE COST ($/kg U)

	Processing	Shipping	U Loss	Totals
Prior to operation				
Transit to conversion		1.68		1.68
Conversion and fabrication *	283		208	491.0
Reactor operation		**	****	
Reprocessing				
Separation	766	**	103	869.0
Conversion to UF_6***	30		35.40	65.40
Transit to AEC ***		0.94		0.94
				1428.02

* Fuel element manufacturing costs included in plant cost rather than fuel cycle because core lasts lifetime of plant.

** Shipment of plant to and from site is charged to capital cost.

*** Burnup on reprocessing availability rate of 200 plants/yr.

**** Burnup cost waived.

(c) Reprocessing

It has been assumed that the plants will be delivered on a periodic schedule. Thus, they will also be ready for reprocessing at approximately the same rate. This will prevent the simultaneous reprocessing of all the spent cores.

Immediate reprocessing of each core as it becomes available would eliminate storage costs. However, processing plant turnaround costs would be lowered by handling a number of plants simultaneously. Obviously, there will be an optimum number of plants per reprocessing cycle to reduce the total cost of the operation. This optimum has been determined as a function of the rate at which the plants are available for reprocessing. As seen in figure 25, a reduction from 200 units per year to 20 would increase fuel cycle costs some 21 percent.

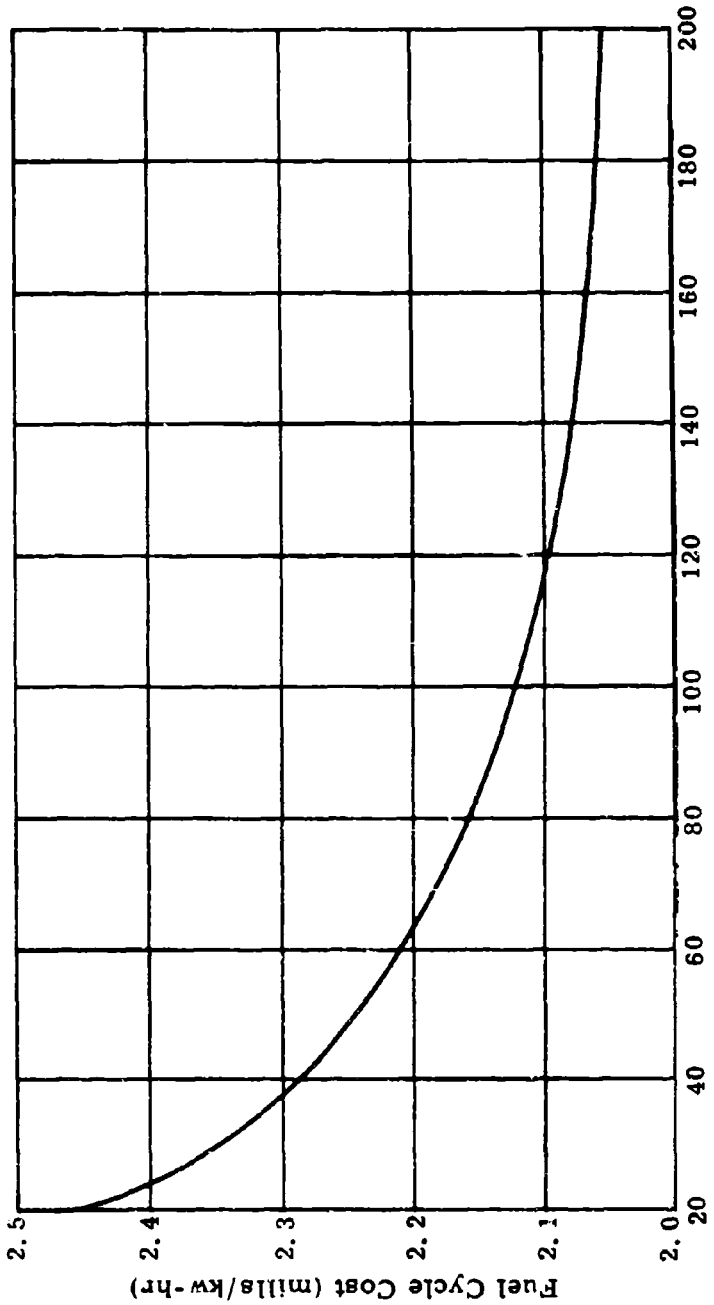

Figure 25. Effect of Reprocessing Rate on Fuel Cycle Cost

This page intentionally left blank.

SECTION IV

REFERENCES

(1) Flynn, G., Percival, W. and Heffner, F. E., "GMR Stirling Thermal Engine, Part of the Stirling Engine Story--1960 Chapter." General Motors Research Laboratories, presented at SAE Annual Meeting, January 1960. SAE Transactions, Vol. 68, 1960.

(2) Personal communication with F. E. Heffner of General Motors Research Laboratories, April 30, 1968.

(3) "Terrestrial Unattended Reactor Power System Analytical Studies." MND-3276, Martin Marietta, May 1967.

(4) Huffman, F. and Biernert, W., "FINK4--A Fortran IV Computer Program for Analyzing Stirling Cycles." MND-3200, Martin Marietta, May 1967.

(5) "Feasibility Study of Control Mechanism and Coolant Properties of a Terrestrial Unattended Reactor Power System." AFWL-TR-67-114, Air Force Weapons Laboratory, July 1968.

(6) Syn, W. and Wyman, D., "DSL Digital Simulation Language--IBM/360 Model 44 User's Guide." 1968.

(7) "Guide to Nuclear Power Cost Evaluation." TID-7025, U.S. Atomic Energy Commission, March 1962.

(8) Nuclear Engineering Handbook, edited by H. Etherington, McGraw-Hill, 1958.

(9) Barrer, R. M., Diffusion in and Through Solids. Cambridge University Press, 1951.

(10) "Data on Diffusion Coefficient of Hydrogen in Copper." Z. Metalls, Vol. 48, pp 373 to 378, 1957.

This page intentionally left blank.

APPENDIX

HYDROGEN REACTIVITY CONTROL (H-RHO)

The principle of H-Rho reactor control is that of reactivity alteration by varying the concentration of hydrogen in the core. A strong negative temperature coefficient of reactivity is created by physically linking the core region to an external source/sink of hydrogen. Materials are selected for each region whose hydrogen contents are an inverse function of temperature and a direct function of pressure. The resulting process is then self-limiting.

The most suitable materials for use in H-Rho are the nonstoichiometric metal hydrides. They offer both high hydrogen densities and a mechanism for effecting sizable changes in hydrogen content. In these compounds, the metals unite with hydrogen, not in specific proportions as they do with many other elements, but in a variable proportion that is a function of hydrogen pressure and temperature. Their behavior in this respect is quite analogous to a solution of a gas in a solid with the exception that the hydrogen densities which can be attained in the nonstoichiometric compounds are orders of magnitude larger than those possible in solutions.

Zirconium hydride is presently the most promising material for use in H-Rho systems. It has already proven to be a successful reactor material in both commercial (TRIGA) and developmental space (SNAP) reactor systems. Other materials such as yttrium and titanium hydrides are strong possibilities, however, these have not been investigated as extensively as zirconium hydride.

1. Examples

An example is given to clarify the H-Rho principle. Figure 26 shows a portion of the pressure-temperature-composition diagram of the zirconium-hydrogen system. Consider an operating reactor in which the neutron moderation is accomplished by zirconium hydride. Assume for simplicity that the hydride is at a uniform temperature and that the hydrogen pressure is maintained constant. Point A in figure 26 represents such a condition where the

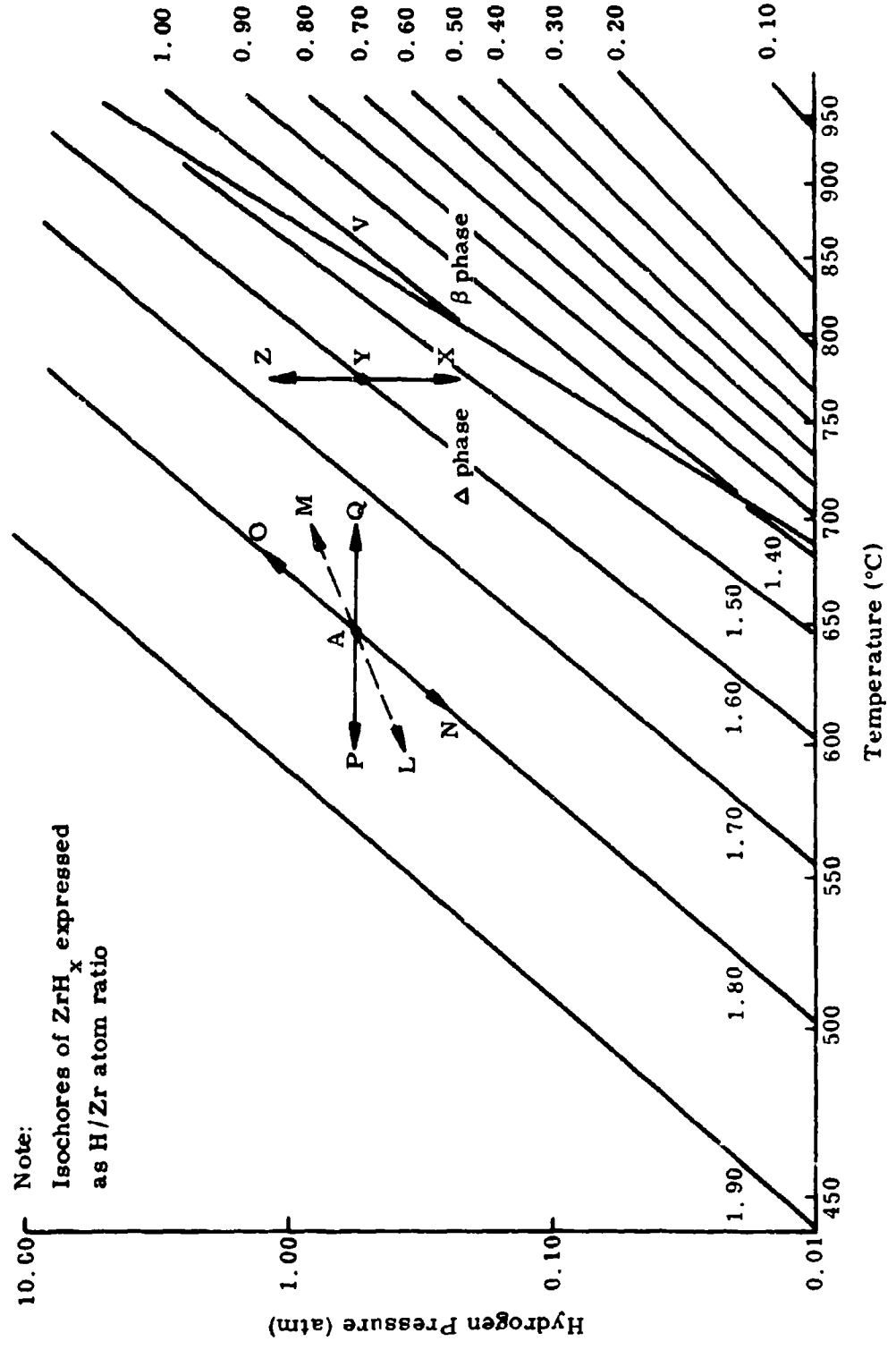

Figure 26. H-Rho Operational Principle with Hydrogen Reservoir

the temperature is 650° C and the pressure is 0.5 atmosphere. Suppose that in response to a power load change, the inlet coolant temperature begins to drop, resulting in a cooling of the hydride material. The operating point will tend to move along the line A-P. As it does, hydrogen is added to the core, as indicated by the increase in the hydrogen to zirconium atom ratio (H/Zr). In a suitably designed core, this increases the reactivity. As the core is now supercritical, power increases to meet the new demand. Eventually, the core will return to its original temperature and hydrogen content at point A. It will again be just critical but the power level will have been increased to match the new thermal load.

As a second illustration, consider the same initial conditions as the previous case. The reactivity of the core is reduced by the accumulation of fission products. The subcritical core will drop in power and temperature, the operating point again moving along the line A-P. Eventually enough hydrogen will be added to restore the core to criticality and a new steady-state will be established at some temperature below 650° C.

These examples, although oversimplified, do illustrate the mechanism by which H-Rho compensates for load changes and reactivity changes, respectively. Other reactivity coefficients affect temperature excursions but do not alter the net result. They merely influence the operating points. Typically, the hydrogen worth is quite large, with the ratio of reactivity change to H/Zr change in the 0.20 to 0.40 range. For a ratio of 0.30, a change of 0.05 in atom ratio will produce a change of 1.5% in reactivity.

Actual temperatures will not be uniform because of heat transfer gradients and power distribution. In a real case, the operating region would be represented by a line rather than a single point. Because there are heat and mass transfer lags associated with any configuration, actual transient conditions will deviate from the equilibrium conditions shown in the diagram. Response times and modes depend on the physical and chemical properties of the system, and these must be carefully selected to attain desired performance levels.

In the examples, it was assumed that the hydrogen pressure was maintained constant. This presupposes the existence of an infinite source/sink of hydrogen. In an actual situation, a finite source/sink, termed the hydrogen reservoir, will be supplied. Hence, the hydrogen pressure will vary as a function of the size, hydrogen content and thermal state of both the core and reservoir. To illustrate, let the state of each section be represented by a point on the pressure-temperature-composition diagram of figure 26. Here the core is represented by point A and the reservoir by point Y. For a constant temperature reservoir, thermal perturbations in the core will cause reservoir movement along line X-Y-Z. Corresponding paths for the core will depend on the size of the reservoir. For one of infinite size we have the case previously discussed. Conditions vary along line P-A-Q. With no reservoir (and consequently no H-Rho) they vary along N-A-O, while for finite reservoirs core conditions would vary along a path intermediate to P-A-Q and N-A-O, such as the dashed path, L-A-M.

It is of interest to note that should the reservoir be operated on the β-δ phase transition line, for example point V, the system will function like the infinite reservoir examples over a rather large range of composition changes.

2. Configuration

A typical H-Rho control system is composed of a fueled core and an unfueled reservoir region, each containing quantities of a metal hydride. An auxiliary heat source (electric heater) maintains the insulated reservoir region at something above the average core temperature. The regions are linked by a gas passage such that chemical equilibrium tends to be established between the two. The core might take on a variety of configurations with a uranium-metal hydride forming the fuel or with a heterogeneous arrangement of hydride and fuel. It might be composed of individual H-Rho elements with separate fuel and reservoir segments or ones that are all interconnected.

3. Operation

The principal operations of the control system include startup, response to temperature changes, response to reactivity changes and shutdown. The accomplishment of each by a typical H-Rho system proceeds as follows:

a. Startup

Utilizing an auxiliary heat source, the reservoir and core are first brought to a temperature where hydrogen transport is rapid enough to provide satisfactory control system response. With the zirconium-hydrogen system, this temperature would be 800° F or higher. Next the reservoir heater is energized. As a temperature difference is established between the core and the reservoir, the core absorbs hydrogen, goes critical and proceeds to match its fission power to the thermal load. The start-up heaters are disconnected and the reservoir heaters switched to plant power. After final adjustment of the reservoir temperature, the system may be left unattended safely.

During the start-up process, the rate at which reactivity is added to the core depends only on the rate of heat input to the reservoir and its heat capacity. These may be established by design, thus eliminating the need to monitor the progress of the startup.

The auxiliary power needed for startup can be supplied either electrically, using a portable power source or chemically, using some convenient exothermic reaction.

b. Response to temperature changes

Once the power input to the reservoir has been set, the reactor will stay critical and supply the thermal power needed to keep at temperature. Any temperature disturbance, whether it be initiated by normal load changes or abnormal accident conditions, will be countered to keep the fuel temperature at its design value. Loss of cooling capacity will result in a shutdown of the reactor. Increase in cooling capacity will be matched by higher power production.

c. Response to reactivity changes

During reactor operation, the hydrogen requirement for criticality is slowly increasing because of fuel depletion, fission product formation, hydrogen redistribution and less significant effects such as core dimensional changes. For a given reservoir temperature, the core temperature declines, allowing more hydrogen to enter. The temperature decline can be kept quite

small through proper core design, which is eased because of the large reactivity worth of the hydrogen.

d. Shutdown

Should the reservoir heater be disengaged for any reason, the core will be set subcritical. For normal shutdown, the heater power circuit would be interrupted. As in the case of startup, the rate of reactivity change is controlled by the heat capacity and heat loss of the system, and no form of external monitor is needed.

4. H-Rho Control Characteristics

Unlike any of the more conventional approaches to reactor control, reactivity can be added to or subtracted from the H-Rho core only as a result of a thermal disturbance or self-induced compositional and dimensional changes. During rapid transients such as load changes or accidents, the former dominates as long as the reactor system remains intact.

The only lag that can exist between a change in fuel temperature and the resulting change in reactivity due to hydrogen transport is that introduced by the mass transfer rate. The analytical and experimental work performed on the transport process has shown that any such lag can be kept small with respect to the heat transfer lag by proper fuel body design. Thus, a practical H-Rho device reacts to transients in much the same way as a reactor with a large negative temperature coefficient of reactivity and possesses the same inherent stability.

A simplified model of the H-Rho system dynamic behavior was used in the design studies of this report. A nuclear reactor represented by the single neutron delay group kinetic equations, controlled only by H-Rho, was depicted. Lumped descriptions of fuel and coolant temperatures and heat transfer were used, and hydrogen transport lag was represented by a single time constant. A linear relationship was assumed between fuel temperature and equilibrium hydrogen content.

The following equations were applied.

a. Coolant heat balance

$$m_c \, cp_c \frac{dTc}{dt} = F (T_f - T_c) - P_L$$

where,

m_c = mass of coolant
cp_c = heat capacity of coolant
T_c = coolant temperature
T_f = fuel temperature
F = heat transfer factor relating the heat being removed from the fuel by the coolant to the fuel-coolant temperature difference
P_L = thermal load on the coolant
t = time

b. Fuel heat balance

$$m_f \, cp_f \frac{dT_f}{dt} = P - F (T_f - T_c) - H \frac{d X_h}{dt}$$

where,

m_f = mass of fuel
cp_f = heat capacity of fuel
P = reactor power
H = heat produced per unit change in X_h from the exothermic hydrogen-zirconium reaction
X_h = hydrogen content of reactor expressed as atom ratio

c. Reactor kinetics

$$\frac{dn}{dt} = \frac{r}{l^*} n - \frac{dC}{dt}$$

$$\frac{dC}{dt} = \frac{\beta}{l^*} n - \lambda C$$

$$P = \frac{P_o}{n_o} n$$

$$r = w (X_h - X_{ho})$$

where,

n = neutron density

r = reactivi'y

1* = neutron lifetime

C = concentration of delayed neutron precursor

β = fraction of delayed neutrons

λ = decay constant of delayed neutron precursor

w = worth of hydrogen per unit X_h

subscript

o = equilibrium conditions

d. Hydrogen equilibrium

$$X_h - X_{ho} = a (T_f - T_{fo})$$

These equations were used to calculate the dynamic response characteristics presented in this report. Previous work[3] indicates that this representation is adequate for the prediction of plant response to normal load changes.

More extensive, detailed analyses of H-Rho control behavior is contained in reference 3. Digital and analog computational techniques are used to provide very accurate description of the H-Rho process during startup and proposed accidental conditions.

UNCLASSIFIED

Security Classification

DOCUMENT CONTROL DATA - R & D

(Security classification of title, body of abstract and indexing annotation must be entered when the overall report is classified)

1. ORIGINATING ACTIVITY (Corporate author)	2a. REPORT SECURITY CLASSIFICATION
Isotopes, Nuclear Systems Division Middle River, Maryland	Unclassified
	2b. GROUP

3. REPORT TITLE

CONCEPTUAL DESIGN STUDIES OF TWO TURPS USING STIRLING AND DIRECT ENERGY CONVERSION CYCLES

4. DESCRIPTIVE NOTES (Type of report and inclusive dates)

June 1968 through March 1969

5. AUTHOR(S) (First name, middle initial, last name)

R. Magladry, G. F. Zindler

6. REPORT DATE	7a. TOTAL NO. OF PAGES	7b. NO. OF REFS
June 1969	96	10

8a. CONTRACT OR GRANT NO. F29601-68-C-0042	9a. ORIGINATOR'S REPORT NUMBER(S)
b. PROJECT NO. 3145	AFWL-TR-68-73
c. Task 24.001	9b. OTHER REPORT NO(S) (Any other numbers that may be assigned this report)
d.	

10. DISTRIBUTION STATEMENT This document is subject to special export controls and each transmittal to foreign governments or foreign nationals may be made only with prior approval of AFWL (WLDC), Kirtland AFB, NM 87117. Distribution is limited because of the technology discussed in the report.

11. SUPPLEMENTARY NOTES	12. SPONSORING MILITARY ACTIVITY
	AFWL (WLDC) Kirtland AFB, NM 87117

13. ABSTRACT

(Distribution Limitation Statement No. 2)

This report presents designs of two compact, unattended nuclear power plants utilizing H-Rho reactor control. One plant is a 100-kilowatt(e) system with Stirling cycle conversion; the other is a conduction-cooled 10-kilowatt(e) thermoelectric system. The conduction system is based upon current technology, while the Stirling system requires an extended life Stirling engine for optimal performance. In addition to the performance the results of parametric studies of system operation at other power levels are included. This report shows that reliable, unattended power can be obtained at moderate cost. The Stirling conversion plant achieves high efficiency and compactness by using the reactor coolant as the engine working fluid. The direct conduction plant provides very long operating life by eliminating moving parts and coolant.

DD FORM 1 NOV 65 1473

UNCLASSIFIED

Security Classification

14. KEY WORDS	LINK A		LINK B		LINK C	
	ROLE	WT	ROLE	WT	ROLE	WT
Advanced low power reactor powerplants Terrestial unattended reactor power system (TURPS) Stirling conversion plant designs Direct conduction plant designs Nuclear Reactor Powerplants						